

Review

Review of the Backfill Materials in Chinese Underground Coal Mining

Junwen Feng^{1,2}, Zhiyi Zhang^{1,*}, Weiming Guan¹, Wei Wang¹, Xinyi Xu¹, Yongze Song¹, Hao Liu¹, Hui Su¹, Bo Zhao¹ and Dazhong Hou¹

¹ School of Geology and Mining Engineering, Xinjiang University, Urumchi 830046, China

² Emergency Management Bureau of Xinjiang Production and Construction Corps, Urumchi 832104, China

* Correspondence: xjuzhiyi@163.com; Tel.: +86-0991-211-1408

Abstract: In China, backfill mining has been selected as an effective approach to realize the green mining of underground coal resources, where backfill materials are the major factor in the development of backfill mining. In order to provide a better reference for further research and development of backfill mining, the experience and research achievements are reviewed in this paper. Firstly, the backfill materials that have been successfully applied in Chinese underground backfill coal mining are divided into two categories according to whether water is used during the backfill mining operation. Then, the primary considerations of each backfill material during its preparation, transportation and activation stages are discussed and evaluated. Finally, suggestions for backfill material exploration are proposed in terms of the future backfill mining of coal resources in Western China, where there is serious surface desertification.

Keywords: backfill mining; backfill material; underground coal mining; green mining



Citation: Feng, J.; Zhang, Z.; Guan, W.; Wang, W.; Xu, X.; Song, Y.; Liu, H.; Su, H.; Zhao, B.; Hou, D. Review of the Backfill Materials in Chinese Underground Coal Mining. *Minerals* **2023**, *13*, 473. <https://doi.org/10.3390/min13040473>

Academic Editor: Abbas Taheri

Received: 21 February 2023

Revised: 13 March 2023

Accepted: 15 March 2023

Published: 27 March 2023



Copyright: © 2023 by the authors. Licensee MDPI, Basel, Switzerland. This article is an open access article distributed under the terms and conditions of the Creative Commons Attribution (CC BY) license (<https://creativecommons.org/licenses/by/4.0/>).

1. Introduction

At the beginning of the present century, green mining, a comprehensive methodological framework, was developed by considering the challenges and advances in Chinese underground coal mining, as shown in Figure 1. Coal is an important fossil resource providing the necessary energy and derivatives for social and economic development, especially in China, accounting for more than 60% of the primary energy consumption [1]. The majority of coal resources are excavated by underground mining rather than surface mining because of the large thickness of the overburden strata and the high complexity of the geological conditions. Extensive underground coal mining inevitably causes many problems. First and foremost, the in situ stress in the surrounding rock around the excavation will redistribute after the coal resource is extracted. As a result, the roof strata over the gob will curve, break and move, and then this kind of strata movement transfers layer by layer from the bottom up and moves gradually away from the disturbance source (i.e., coal face) until a new balance both in the stress and structure is achieved. During these adjustments of the stress and rock structure, a series of problems will often be encountered, including gas release and explosion, groundwater recession and inrush, surface subsidence and construction damages [2]. Secondly, coal gangue will also be produced during underground coal mining resulting from a large number of roadways in the rock strata that have to be excavated for the purposes of transportation and ventilation. A large amount of coal gangue deposited on the ground surface not only causes air pollution on account of spontaneous combustion but also occupies farmland owing to gangue dump disposal [3]. Last but not least, a certain amount of coal will be leftover during mining processes, such as coal pillar supports, broken coal loading and transportation. The coal left underground can itself likely combust as well and thus trigger a fire hazard [4]. Additionally, coal waste because of coal pillar supports always contributes to the low coal resource recovery in

China [5]. The abovementioned challenges associated with underground coal mining result in serious personal casualties and property loss. In recent decades, the increasing social concern regarding ecological and health risks has led to the implementation of more advanced mining technology and theory in underground coal mining. In 2003, based on a comprehensive consideration of the challenges and progress of underground coal mining in China, Qian et al. proposed a green mining concept aimed at solving the abovementioned series of challenges arising from underground coal mining in which backfill mining can minimize mining-induced hazards and maximize the recovery of coal resources. [6].

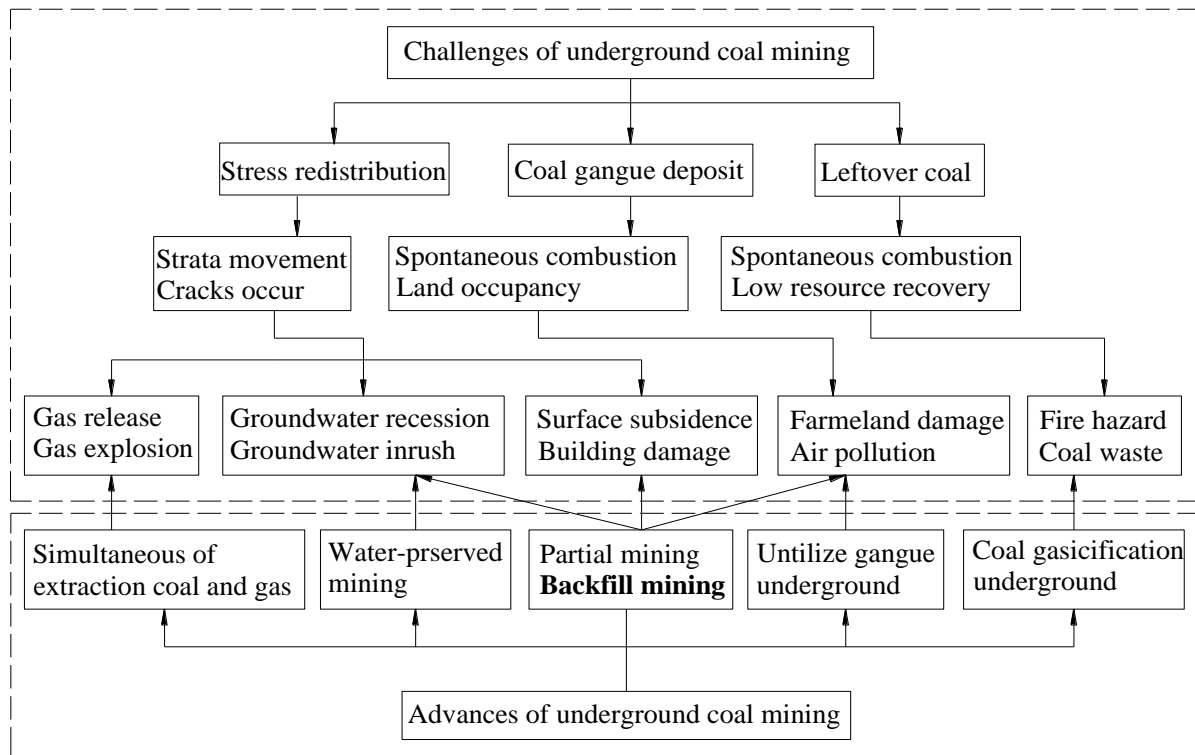


Figure 1. The theoretical and technical framework of underground coal green mining [6].

Backfill mining is the most effective approach for realizing the green mining of underground coal resources. Longwall mining has become the most common underground coal-mining method in China in recent decades due to its optimal performances in large productivity and high efficiency [7]. Experience indicates that the major concerns of an underground longwall mining disturbance are the extent of the surface subsidence and the resulting surface structural damage; breakage of the water-bearing strata, ground and water recession; the appearance of cracks in the surrounding rock and triggered gas release, since there is a complete extraction of the coal in a longwall panel, as shown in Figure 2a. In dealing with coal resources under special conditions where a large surface subsidence is not allowed, such as in construction, railways and water bodies, conventional longwall mining will not qualify. Partial mining methods, including room and pillar mining, strip mining and limited thickness mining, were designed to extract the underground coal seam under the aforesaid special conditions, as shown in Figure 2b. When the movement of the overburden strata is limited through considerable coal pillar support, coal resource recovery decreases immediately, and stress concentrations, such as gas outbursts, and mine fire hazards are caused indirectly. In order to eliminate the risks associated with these conventional mining methods and to also increase the coal recovery, backfill mining was selected as the most appropriate choice, as shown in Figure 2c. On the one hand, the gob space can be filled with the backfill material, thereby limiting the overburden strata movement to within an acceptable level [8]. On the other hand, the coal pillar left for

supporting the overburden strata in the partial mining could be replaced completely by the backfill mass and, consequently, the recovery of coal resources can be maximized [9]. Furthermore, the coal gangue originally causing air pollution and farmland occupation could be backfilled in the gob [10]. As a result, the majority of the risks resulting from underground coal mining can be perfectly resolved. At the same time, backfill technologies are perfect for the placement of waste, which is a desirable phenomenon for environmental reasons. Korzeniowski et al., focusing on the increasing amount of waste residue generated by municipal solid waste incineration (MSWI), carried out a large number of attempts to fill the goaf [11]. Skrzypkowski et al. added flue gas treatment solid waste and fly ash to backfill materials to explore the compressibility of backfill [12].

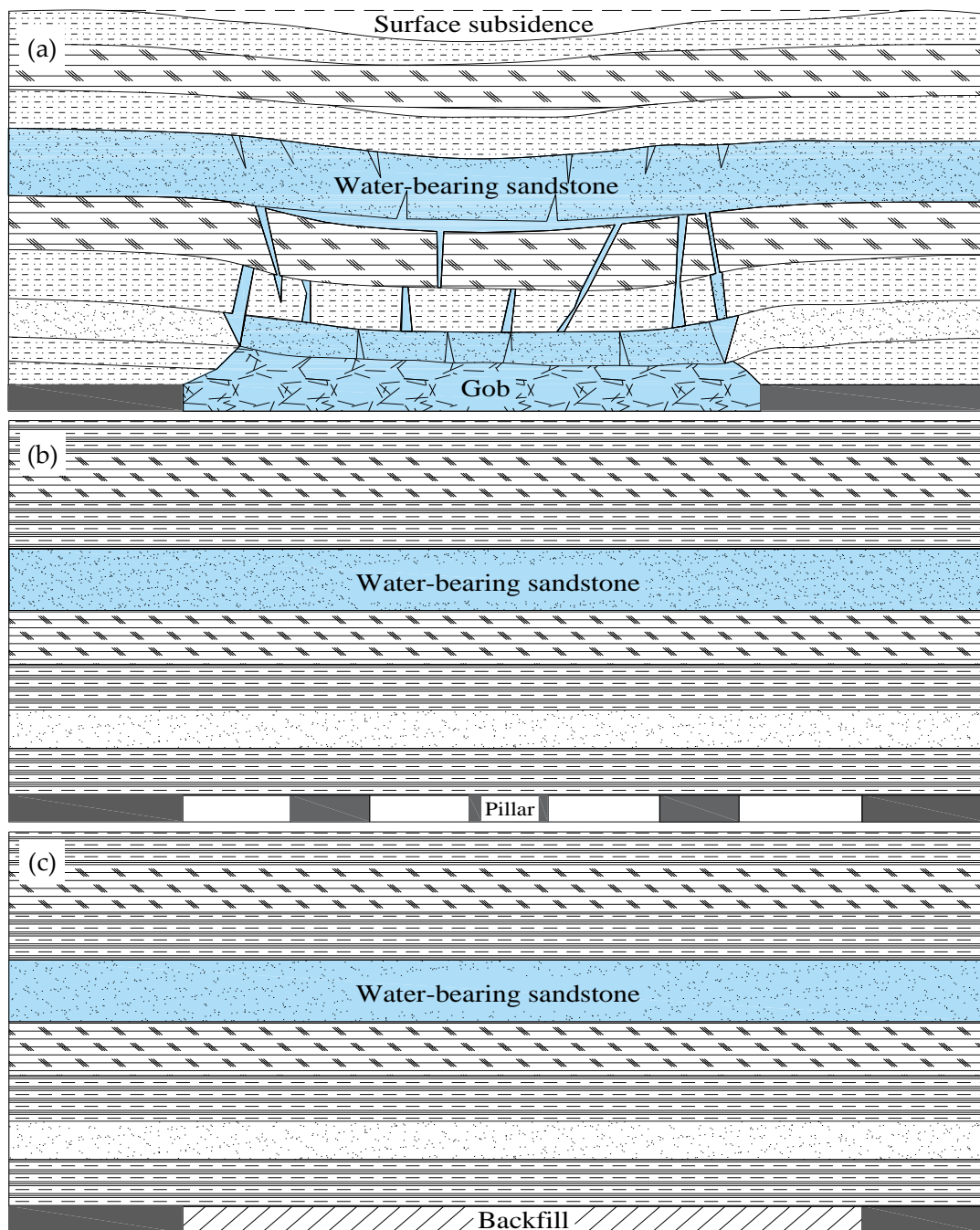


Figure 2. Overburden strata movement with different underground mining methods: (a) natural caving method; (b) partial mining method; (c) backfill mining method.

Backfill material has the most responsibility for the promotion of backfill coal mining. In order to realize the predicted increase in the recovery of coal resources and the decrease in mining-induced environmental impacts, the backfill material must satisfy strict requirements, including economical reasonability and technical feasibility [13]. Firstly, considering the fact that coal is not as expensive as metal minerals per unit, the material backfilled in an underground coal mine should be much cheaper than those used in a metal mine to make the coal-mining activity profitable. Statistically, as much as one-third of mining costs can be attributed to the investment in the backfilling of coal mines, where the cost of the backfill material accounts for more than 80% [14]. In addition, there is no sufficient ready-made powdery material in coal mines as in metal mines (generated by the milling process); thus, the selection of an economical backfill material within the size limit of coal mines is a more challenging task. Secondly, the overburden strata of a coal seam usually consist of sedimentary rock with lower strength than the magmatic rock and metamorphic rock in a metal mine and, therefore, the roof strata over a coal mine's gob always curve and cave more easily than those over the gob in a metal mine. The material backfilled in an underground coal mine should acquire a larger mechanical strength within a shorter time so as to bear the overburden stress and limit the overburden strata movement effectively. Commonly, a proportionality relationship is shown between the performance and the cost of the backfill material; a compromise between these two indexes of the backfill material should be determined in practice. Additionally, backfilling procedures such as backfill material preparation, transportation and activation also have to be adjusted accordingly to satisfy different characteristics of the final selected backfill materials. Therefore, the selection of an appropriate backfill material for an underground coal mine has become the key to backfill mining to a large extent.

In China, backfill material employed in underground coal mines is divided into two categories: water-involving backfill material and waterless backfill material. By now, the locations of the underground coal mines extracted through the backfill mining method are mainly distributed in Mideastern China (Shandong Province, Shanxi Province, Henan Province, etc.), as shown in Figure 3, where the contradictions between mining activities and environmental protection are the most unreconciled due to the impressive demand for coal energy and the urbanization process. The mideastern provinces remain the primary locations responsible for the supply of energy for national socialization from the beginning of the establishment of China [15]. According to statistics, the amount of coal reserves that need to be extracted using the backfill mining method is as much as 13.79 billion tons in Mideastern China, and the parts beneath construction projects, railways and water bodies account for approximately 60%, 20% and 20%, respectively [16]. Importantly, the amount of coal under special conditions is increasing gradually over time. It can also be seen from Figure 3 that all of the materials applied in Chinese underground backfill coal mines mainly comprise four types, including hydraulic backfill material, cemented backfill material, gangue backfill material and high-water backfill material. These backfill materials can be further divided into two categories, including water-involving backfill materials and waterless backfill materials, depending on whether water is used during the backfill mining operations.

Analyzing the above, it can be noted that reducing the environmental damage caused by coal mining via gob backfilling is a very topical issue. The backfill material has the most responsibility for the promotion of backfill coal mining. Therefore, the purpose of this study was to provide valuable references for the world's main coal-mining countries in the exploration of appropriate backfill materials through a comprehensive review of the experiences in Chinese backfill mining. To achieve this goal, the following questions needed to be addressed: (1) What are the backfill materials that have been successfully used in China? How can these backfill materials be classified? (2) What are the advantages and disadvantages of the different types of backfill materials? How can the appropriate backfill materials be selected to satisfy the different backfilling stages?

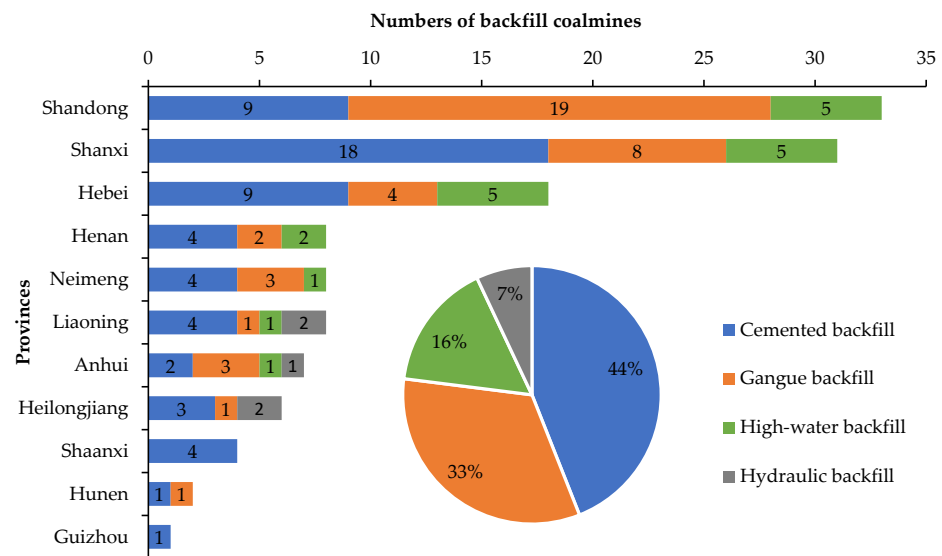


Figure 3. Distributions of backfill coal mines and backfill materials in China (all data are from the China National Knowledge Infrastructure).

2. Water-Involving Backfill Material

2.1. Hydraulic Backfill Material

Hydraulic backfill mining is the earliest backfill mining method that is largely employed in Chinese underground coal mining, as shown in Figure 4. This backfill mining method was first proposed in America for the purpose of protecting a church located above an underground coal mine. After, this mining method was introduced in Europe, and it was especially largely popularized in Poland. As of 1960, Chinese mining engineers started to import this mining method to extract metallic mineral resources, and the backfill material mainly consisted of powdery tailings from solid ore milling operations [17]. It has been found that this mining method can effectively limit the overburden strata’s movement. Shortly afterward, hydraulic backfill mining was successfully employed to extract underground coal resources in cases where villages were located above. As shown in Figure 4, solid aggregate is first mixed with water, the slurried material then flows into the underground gob space and, finally, the water is exuded from the hydraulic fill; the solid aggregate left in the gob can fill the excavations and limit the potential movement of the overburden strata. The water that exudes from the gob has to be pumped up to the water sump at ground surface, where the mud in the dirty water will be removed through a precipitation process, and the clean water can be reused in the next backfilling cycle.

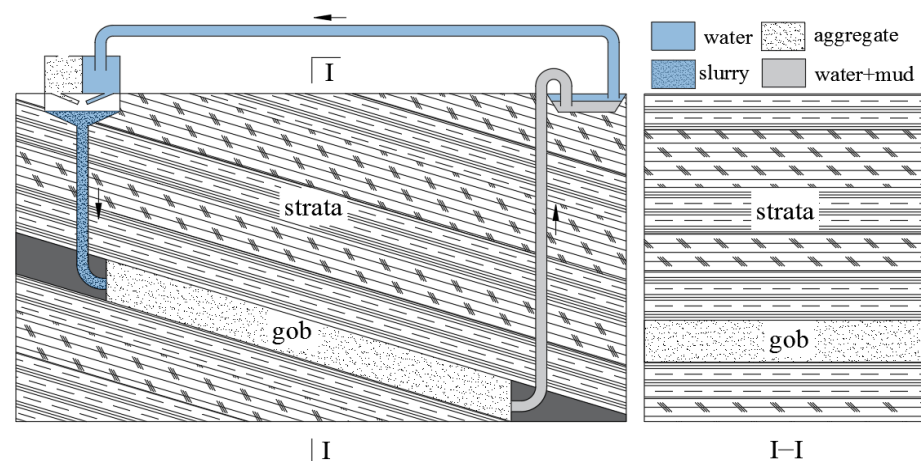


Figure 4. Hydraulic backfill mining system.

2.1.1. Preparation of Hydraulic Backfill Material

The hydraulic backfill material selected for underground coal mining is always composed of water and solid aggregate, including gangue, sands, gravel and other solid construction wastes. It should be noted that the main purpose of water during the preparation process is to make the material flowable to facilitate the following transportation operation. The addition of water in the backfill material acts like a “carrier” for the solid aggregate and does not react with the solid aggregate. The solid aggregate is the main load-bearing structure of the backfill material, and the grain size and grading type have to be taken into consideration during the preparation process to ensure that the hydraulic backfill material is sufficiently fluxible in the pipeline during the transportation stage and to provide it with sufficient strength in the gob space during the activation stage [18].

2.1.2. Transportation of Hydraulic Backfill Material

The hydraulic backfill material (i.e., solid aggregate) is mixed with water and, thus, floats in the slurry, resulting from the buoyancy force of the water before transportation. At the same time, the solid aggregate in the slurry also sinks toward the pipe shell due to the fact of its own gravity. As a consequence, the solid aggregate will settle during transportation and can only move a certain distance with the flowing water, as shown in Figure 5. Apparently, the transportation distance of the solid aggregate during hydraulic backfilling mainly depends on the amount of time that the solid aggregate takes while maintaining a floating state in the slurry. Unfortunately, the suspension time of the solid aggregate in water is always limited, because the downward gravitational force imposed on the solid aggregate is much larger than the upward buoyancy force on them due to the fact that the density and size of the solid aggregate in hydraulic backfilling are always large [19]. The fluid mechanics equation of the solid aggregate during hydraulic transportation is as follows:

$$F = (\rho_1 - \rho_2)gV \quad (1)$$

$$G = ma \quad (2)$$

$$F = G \rightarrow a = \left(1 - \frac{\rho_2}{\rho_1}\right) \quad (3)$$

where ρ_1 is the density of the solid aggregate, ρ_2 is the density of the water, V is the volume of the solid aggregate, m is the mass of the solid aggregate and a is the vertical accelerated speed of the solid aggregate.

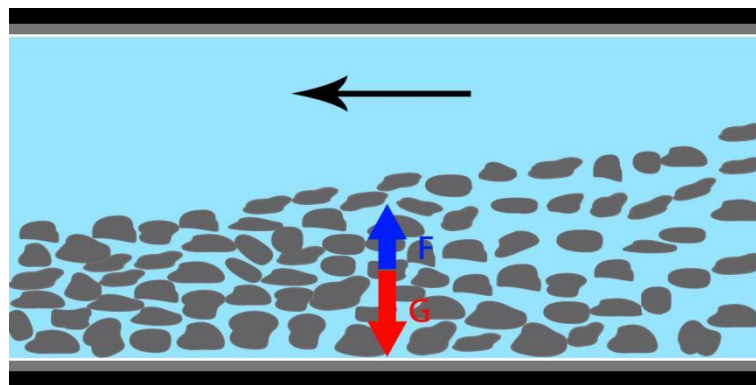


Figure 5. Forces imposed on the solid aggregate during transportation.

An important parameter, which is closely related to laboratory tests, is the diameter of the sand grains, which is taken into account in the calculation of the critical velocity and the motion confidence index of the backfilling mixture. While the water itself can flow at a

very low velocity, a flow velocity greater than the so-called critical velocity below which the solids begin to settle is necessary to keep the solids suspended in the water.

The critical velocity (c_v) of the flow-filling mixture, taking into account the kinetic specific gravity of the feed and the maximum grain dimensions (N/m^3), is expressed by Equation (4) [20]:

$$c_v = \frac{-8.491}{d + 1.284} + 5.04 \quad (4)$$

where d is the maximum grain size (mm).

2.1.3. Activation of Hydraulic Backfill Material

The mechanical strength of the hydraulic backfill material is achieved through the friction and squeezing between the solid aggregate particles left in the gob after segregation. At the beginning of the activation stage, the gob is almost fully filled by the mixture of water and solid aggregate, as shown in Figure 6a. Then, the water content in the mixed slurry will gradually exude out, and the solid aggregate particles left in the gob are driven by their own weight to come into contact with each other [21]. Apparently, an empty space appears again between the roof and the fills due to water bleeding, and a certain number of interspaces still exist between the solid aggregate particles, as shown in Figure 6b. After, the overburden strata will sink and compress the aggregate particles, and the friction and squeezing force between the contacted particles will be enhanced. Consequently, an upward force is produced, which limits the further sinking of the overburden strata, as shown in Figure 6c. At the end of the activation stage, the bearing strength of the backfilled mass increases sharply, resulting from the fact that the internal voids between the particles are compressed increasingly smaller by the sink movements of the overburden strata. The movements of the overburden strata will finally stop when the upward bearing strength of the fills equals the downward compressing stress of the overburden strata and, meanwhile, the compactness of this backfill material reaches its maximum value.

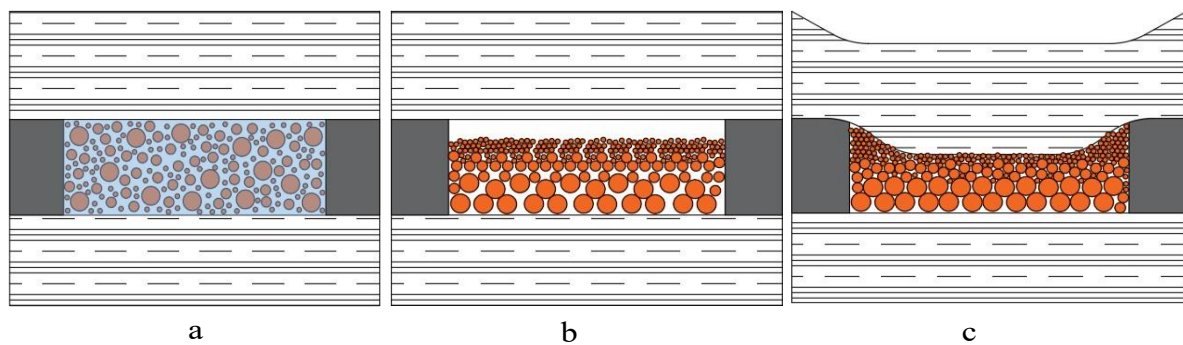


Figure 6. (a) Beginning of activation; (b) middle of activation; (c) end of activation of the hydraulic flushing backfilling material.

Theoretically, the smaller the grain composition of the solid aggregate particles, the smaller the initial interspaces in the backfill material, the less the volume shrinkage and the better the control effect on the overburden strata's movement [22]. Unfortunately, small initial interspaces mean a low water permeability in the backfill material, which indicates that a much longer time is needed for water to bleed completely. As a matter of fact, a balance between the porosity and compactibility of the hydraulic backfill material becomes the primary consideration for engineers to achieve an expected backfill result in its application in the field. Practice has proved that water permeability within a magnitude of 1×10^{-5} – 1×10^{-6} m/s is commonly appropriate for underground coal backfill mining with a coal production of no more than 0.3 Mt/a [23]. Furthermore, studies have indicated that the water permeability can be increased by decreasing the number of small-sized fine particles through desliming and hydrocyclone operations, and the compactibility can be improved by increasing the number of middle-sized sand particles in gravel-based hydraulic

backfill material [24]. It should also be noted that small-sized particles in hydraulic fills will migrate toward the direction of the exuding water, and the coarse particles always transfer backward in the direction of the exuding water during the segregation and consolidation processes of the hydraulic fills in the gob. As a consequence, the final particle distribution and resulting voids, porosity, density and mechanical properties exhibit an obvious layered anisotropic phenomenon, to which should be attached more importance for the purpose of achieving a better comprehensive understanding of the bearing mechanism of hydraulic fills during the activation stage in the gob [25].

2.1.4. Time Needed to Fill the Post-Mining Space with Hydraulic Backfill Material

Filling the goaf with hydraulic backfill material is usually quite time consuming. In order to ensure that the hydraulic backfill material can be transported successfully from the ground to the goaf, a large amount of water is added to the filling material and injected together with the filling aggregate into the goaf at the initial stage of filling, which requires the construction of a large number of artificial water-plugging facilities at the goaf boundary [19]. However, the water that enters the goaf with the aggregate needs to be completely removed from the goaf during the activation stage of the hydraulic backfill material, which also requires the construction of a large number of artificial water filtration facilities [23]. In addition, the water from the goaf needs to be collected again and pumped to the surface for filtration and reuse. All of these water-related operations make it difficult for the hydraulic backfill material to completely fill the gob, and the filling rate is too slow to match the faster mining speed.

2.1.5. Evaluation of Hydraulic Backfill Material

Advantages: Firstly, the requirement for the backfill material is easily satisfied and, thus, almost all the solid waste and natural gravel within a size limit can be flushed hydraulically into the underground gob to support the overlying strata. Consequently, the cost of the backfill material's preparation is favorable. Secondly, the skill requirement for the backfilling operation is relatively low, and miners can operate the backfilling equipment and complete the backfilling process without intensive training. As a result, the backfilling system is reliable and easily carried out.

Disadvantages: Firstly, the transportation efficiency of the backfilling material is low due to the fact the mixed slurry always encounters segregation easily during the transportation process. The solid aggregate cannot be transported any further through the pipeline without floating in the water. Secondly, the activation efficiency is low because the water bleeding during the activation stage in the gob is fairly time consuming and, thus, a relatively long time must be spent for the slurried material's consolidation. In addition, the water recycling is also complicated, because the fine particles (i.e., mud) exuded together with water from the initial hydraulic fills have to be removed in the settling pond before the water is reused in the next backfilling cycle. As a consequence, the slow backfilling procedure cannot match the increase in the moving speed of the coal-mining face. Thirdly, the control effect on the overburden strata movement is unachievable, obviously because the gob space is always difficult to be fully filled by this slurried material due to the fact that a large amount of free water flows away from the gob during the activation stage. Additionally, the thickness of the loose aggregate after water bleeding will also be compressed further by 10%–20%. Therefore, the subsidence coefficient of the ground controlled by this hydraulic backfill material is commonly kept within a range of 0.1–0.3 [26,27]. Last but not least, the cost of recycling the water, removing the fine particles and constructing a waterproof floor and water-permeable walls also weakens the economic feasibility of this backfill mining method.

2.2. Cemented Backfill Material

Cemented backfill mining is the second backfill mining method that is largely employed in Chinese underground coal mining, as shown in Figure 7. The most significant

improvements in the cemented backfill material compared with the hydraulic one is that the slurry concentration is increased and the water bleeding time is shortened by introducing a cementing agent [8,28]. Cemented backfill mining was first proposed in Austria and Canada to replace the previous hydraulic backfill mining [29,30]. In the 1970s, this modified backfill mining method was introduced in China, and it was similarly applied in underground coal mines after the practices in metal mines achieved success [31]. After, the concentration of the cemented backfill material continually increased to improve the material's flow property and consolidation strength. In 2006, a modified cemented backfill material, a pasty slurry, was tested in a Taiping coal mine, indicating that cemented backfill mining in China has entered a new advanced stage [32]. Practice indicates that this modified backfill material's performance has obvious advantages, including high efficiency during the transportation stage and large bearing strength during the activation stage [33–35]. Most importantly, the water constituent added during the slurried material preparation stage can react with the cementing agents during the activation period in the gob and, thus, no surplus water exudes out from the gob space [8,36]. Therefore, costs for the drainage of the water and fine particles can be saved, the backfill mining speed can be accelerated, the gob space can be fully filled and the control effect on the overburden strata can be guaranteed as well [37–39].

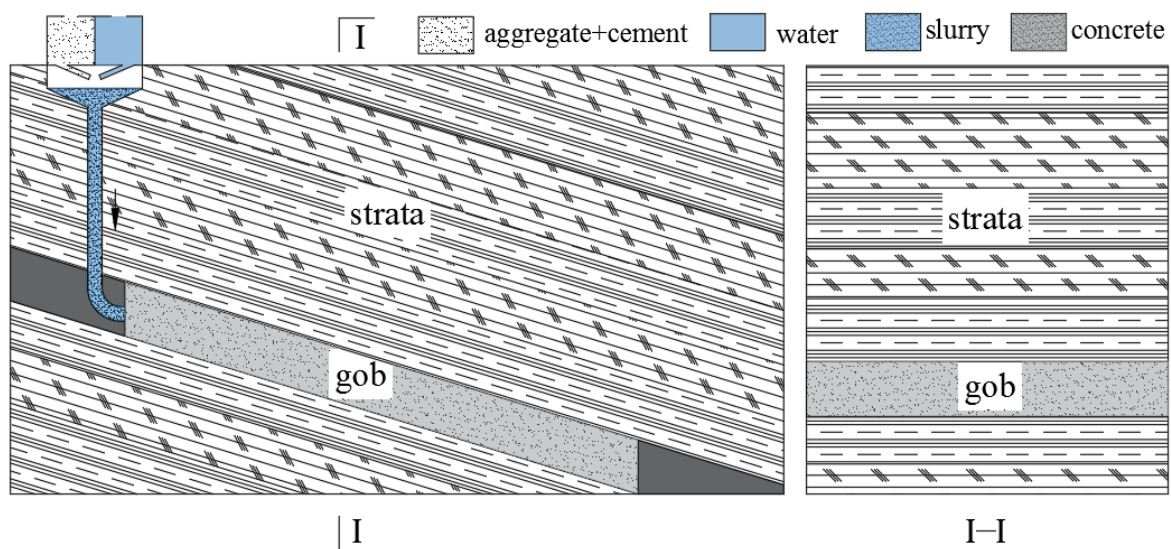


Figure 7. Cemented backfill mining system.

2.2.1. Preparation of Cemented Backfill Material

The cemented backfill materials used in underground coalmines commonly consist of water, cementing agents and coarse and fine aggregates, and the percentages of each are illustrated in Figure 8. The solid coarse aggregates are usually composed of cracked gangue, solid construction waste and gravels; the solid fine aggregates are mainly composed of coal gangue, tailings and sand (river sand and aeolian sand) and the cementing agents are mainly made from coal ash, Portland cement, gypsum and lime. It should be noted that the majority of the water added during the preparation stage not only plays a role in reducing the transportation resistance by floating the solid aggregate away from the pipeline's wall but also increases the final consolidation strength in the gob through a chemical reaction with the cementing agent [40–42].

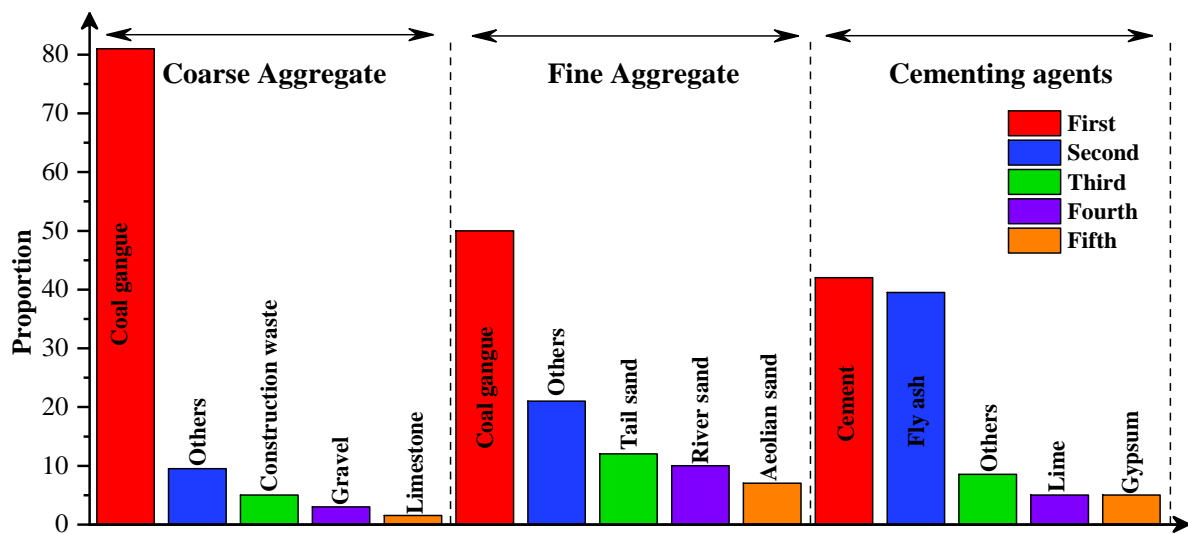


Figure 8. Percentages of the different participants in cemented backfill material.

Coal gangue: The most common coarse aggregate in the cement filling material is coal gangue. It is the incombustible rock mass produced during underground coal mining processes, such as the coal cutting procedure at the coal mining face and the blasting procedure at the roadway driving face [28,43]. According to statistics, the quantity of coal gangue comprises approximately 30% of the whole coal production in China, with more than 60% coming from the coal preparation procedure [44,45]. The original coal gangue is always large in size and of poor grading, and it should be cracked to an appropriate lumpiness to facilitate the following transportation and activation processes [46]. An SEM image of coal gangue is provided in Figure 9a.

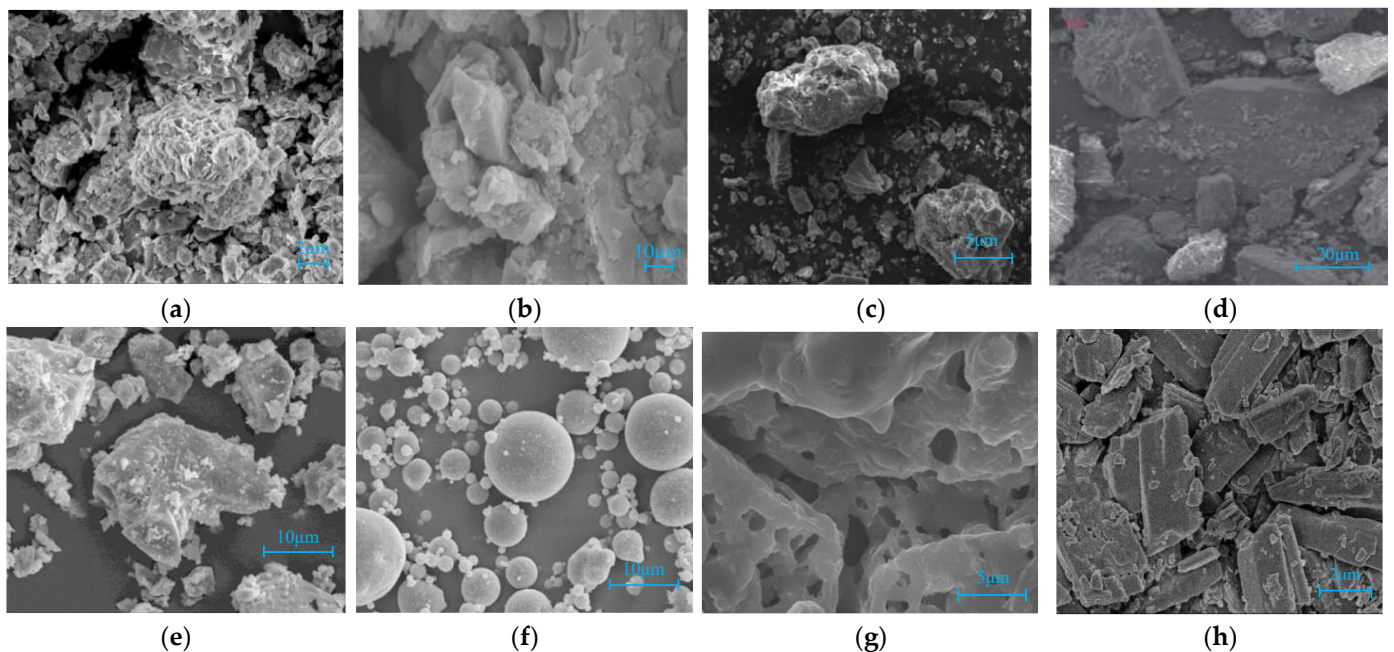


Figure 9. SEM images of the cemented backfill material [37,47–50]: (a) coal gangue magnified by 5000×; (b) limestone magnified by 4000×; (c) tailings magnified by 5000×; (d) river sand magnified by 4000×; (e) magnified Portland cement; (f) magnified coal ash; (g) magnified lime; (h) magnified gypsum.

Tailings: Tailings are powdery rock masses that are mainly generated from the milling process in metal mines. Tailings are the main solid waste of metal mines. Tailings are the ideal fine aggregate of cemented backfill material because their particle size matches the requirement of backfill material. However, the mud component of tailings has a negative influence on the mechanical strength of solidified backfills in the gob during the activation stage [51]. An SEM image of tailings is provided in Figure 9c.

River sand and aeolian sand: Natural sand is the result of the long-term collision and friction of gravel particles; the former is driven by the force of flowing water in rivers, and the latter is driven by the force of blowing wind in the air [52]. The particles of river sand are angular and outstanding in grading, which makes this kind of material a perfect selection for the fine aggregate constitute of concrete not only for underground backfilling but also for surface construction. However, the production of river sand is always limited and, most importantly, the mining process of river sand damages the environment as well. Compared with river sand, aeolian sand is much more easily accessed, and the quantity of aeolian sand is much larger. However, aeolian sand is characterized by regionalism and is mainly distributed in the northwest of China, where a large area of desert is located. Fortunately, approximately 50% of the coal reserves in China are distributed there, and aeolian sand could be an ideal choice for the fine solid aggregate selection when the cemented backfill mining method is employed to extract underground coal reserves [53]. The particle size of aeolian sand is uniform, and more than 80% of particles have a grain diameter between 0.1 and 0.25 mm, affecting the mixed backfill materials greatly both in the transportation stage and activation stage [54]. An SEM image of river sand is provided in Figure 9d.

Portland cement: Portland cement is made according to the following sequence. Calcareous and aluminosilicate raw materials are mixed in a certain proportion and then ground and calcined at high temperature (about 1720 K) to obtain clinker. Finally, it is ground together with an appropriate amount of gypsum to a certain fineness. The main particle size of Portland cement is 20–80 μm , the minimum particle size is 2 μm and the maximum particle size is 285 μm [51]. An SEM image of Portland cement is provided in Figure 9e.

Coal ash: Coal ash refers to the matter collected from the flues of coal-fired power plants after coal combustion in a boiler [55–57]. The coal ash that is finally formed (80~90% is fly ash and 10~20% is furnace bottom ash) is a complex and variable multiphase substance with a similar appearance and fine and uneven particles [37,50]. The types of coal, fineness of coal powder, combustion and collection methods of coal ash always cause many differences in the chemical properties of coal ash. The main chemical composition of coal ash, however, is basically unchanged. Its chemical composition mainly includes SiO_2 , Al_2O_3 , Fe_2O_3 , CaO and MgO ; the main mineral components of coal ash are quartz and mullite and the content of quartz is the largest [52,53,56,58,59]. The particle size of coal ash is 3~350 μm , and its main particle size is 10~60 μm . Approximately 50% of the particles are sized less than 30 μm , and 80% of the particles are sized less than 100 μm . The SEM figures show that a large number of spheroid glass beads with a smooth surface and compact size can be seen under high magnification, the particle sizes of which ranged from 1 μm to 30 μm . The glass beads are independent of each other or aggregate into large particles. There are some amorphous flocculent coal ash gelation and acicular mullite on the surface of the coal ash particles, and the surface of the large coal ash particles is uneven with a large number of holes [39,52]. An SEM image of coal ash is provided in Figure 9f.

Lime: Lime is a kind of gaseous inorganic cementitious material with calcium oxide as the main component. Lime is made of limestone, dolomite, chalk, shell and other products with a high calcium carbonate content, calcined at 900~1100 $^\circ\text{C}$. The chemical composition of lime is CaO , Al_2O_3 , Fe_2O_3 , SiO_2 , MgO , Na_2O and K_2O [60]. The microscopic morphology of the lime samples was analyzed by field emission scanning electron microscopy (SEM), as shown in Figure 9. It can be seen that the pores of the lime are narrow and small, the number of pores is small, there are floccule substances on the surface of the particles, the

particles are not uniform in size and the particles are loose. The SEM images of the lime and limestone are provided in Figure 9b,g.

Gypsum: β -Hemihydrate gypsum is obtained after desulphurized gypsum is heated to 110–170 °C in dry air. Most of the gypsum employed in Chinese underground backfill mining is β -hemihydrate gypsum. The chemical composition of gypsum mainly consists of CaO, SiO₂, Fe₂O₃, Al₂O₃, MgO, CaSO₄, etc., and the main components of gypsum are 2CaSO₄·H₂O and SiO₂ and the content of 2CaSO₄·H₂O is the largest. The microscopic morphology of gypsum samples was analyzed using field emission scanning electron microscopy (SEM), as shown in Figure 9. It can be seen that the gypsum is mainly rod-shaped crystals with a large length-to-diameter ratio. The gypsum crystals are well developed, the particles are generally fine and uniform and the impurity particles attached to the surface of the particles are fewer. The SEM images of the gypsum are provided in Figure 9h.

2.2.2. Transportation of Cemented Backfill Material

As mentioned above, water–sand filling slurry is a typical two-phase flow. In the transportation process, aggregate with a large particle size is easily precipitated due to the fact that the downward gravitational force is greater than the upward buoyancy force, which easily blocks the transportation pipeline and cannot achieve the purpose of long-distance and efficient transportation. Therefore, increasing the buoyancy of the coarse aggregate in slurry is an effective way to avoid premature precipitation. The buoyancy of the aggregate in slurry is mainly controlled by the slurry viscosity, and the fundamental method to increase the slurry viscosity is to increase the interaction force between the different molecules in the slurry [61,62]. Based on this, large numbers of microparticles have been added to the cemented slurry. Microparticles mainly include cement and fly ash. With the increasing proportion of these microparticles, the transportation concentration of cemented filling slurry gradually increases, and the rheological properties of the slurry during transportation are also significantly improved [59].

In cemented filling slurry, intermolecular forces contributing to the slurry viscosity mainly include the interaction force between water molecules, the interaction force between water molecules and microparticles and the interaction force between adjacent microparticles.

The interaction force between water molecules: The fine aggregate particles in the cemented slurry are uniformly suspended in the slurry solution rather than dissolved in the slurry solution. Therefore, the addition of fine aggregate does not change the interaction force between the water molecules.

The interaction force between water molecules and solid particles: Physical force—surface energy is usually found on the surface of microparticles, and the larger the specific surface area, the higher the surface energy. The higher the specific surface energy of a particle, the more unstable the particle surface becomes, and the surface energy eventually tends toward a lower stable state. Microparticles added in slurry usually reduce their specific surface energy by adsorbing water molecules to reach a stable state. The larger a microparticle's specific surface area, the stronger the adsorption capacity of the water molecules. Chemical force—chemical adsorption is mainly attributed to the fact that the Si-O-Si and Al-O-Al keys on the surface of microparticles have positive electricity. At the same time, a water molecule is a dipole characterized by an asymmetric positive charge performing uneven distribution around negative charges, and both have their own charge centers and their effects cannot cancel each other out. Oxygen needs electrons more than hydrogen does (a property called electronegativity). In other words, when hydrogen and oxygen bond, the covalent electrons travel mostly around the negatively charged oxygen. So, the oxygen side of the covalent bond is negative, and the hydrogen side is positive. As a result, the positive charge on the solid microparticle's surface attracts the oxygen atoms of the water molecule, and an adsorbed water film forms on the surface of the microparticles, as shown in Figure 10a.

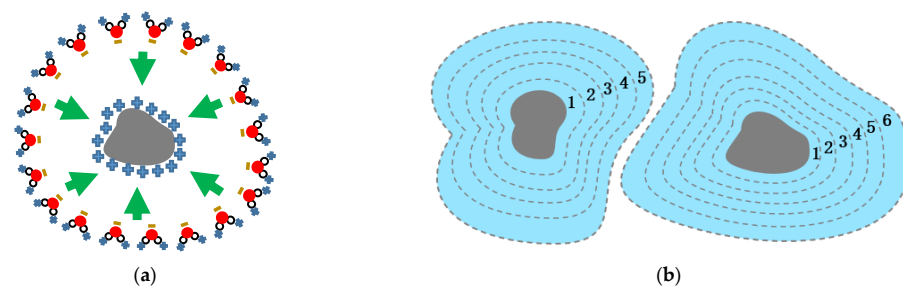


Figure 10. (a) Adsorption between water molecules and micro solid particles; (b) water film around micro solid particles.

According to Coulomb's law, the electric field intensity is inversely proportional to the square of the distance. Therefore, water molecules close to the microparticle's surface are strongly attracted by electrostatic force. As the distance increases, the attraction force decreases. The bound water formed on the surface of particles can be divided into strongly bound water located at the inner layer and weakly bound water located at the outer layer. Therefore, after intense agitation, good contact between the microparticles and water molecules is achieved, and a large number of water molecules will be adsorbed on the surface of the microparticles, forming multilayer water films, as shown in Figure 10b. The particles have stronger adsorption on the nearby water film and do not easily break away from the bondage of the particles. However, the water film that is far away from the microparticles easily escapes from this bondage due to the fact of its relatively weak adsorption capacity. In addition, the existence of water film increases the volume of the microparticle equally, thus further increasing the buoyancy force of the microparticles [63]. On the other hand, due to the existence of water film on the surface of the microparticle, the proportion of bound water is increased, the proportion of free water is reduced and the utilization efficiency of the water is improved.

The interaction force between micro solid particles: As mentioned above, water film will be adsorbed around the microparticles because of the high specific surface energy. Microparticles can react with each other through the Van Der Waals force of the water film located between them. Consequently, the spacing between microparticles becomes smaller, and the interaction between the particles becomes stronger.

In summary, the interaction force between molecules in the slurry prevents the dislocation between molecules, as shown in Figure 11a. When particle 2 tries to dislocate upward, this kind of movement will be limited by the following three forces: firstly, the coulombic force between particle 2 and adjacent particles; secondly, the coulombic force of the water film of particle 2 and adjacent particles and, third, the Van Der Waals force belonging to two adjacent particle water films. These forces prevent the movement of particle 2 and keep particle 2 in a stable suspended state [64], as shown in Figure 11b.

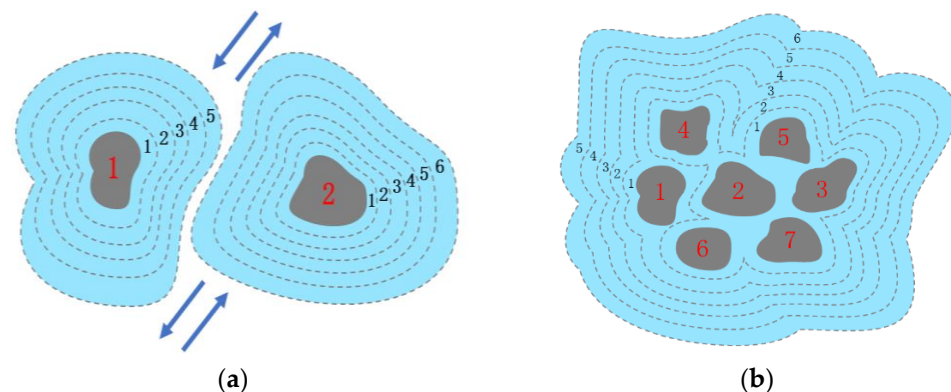


Figure 11. (a) Flocculation network structure in cemented slurry; (b) suspension mechanism of small solid particles in cemented slurry.

As for the microparticles in a suspension liquid, the difference between the gravity and buoyancy is no longer distinct. Taking all influencing factors into consideration, the settlement velocity of fine aggregate particles in cemented filling slurry conforms to the following formula:

$$6\pi r_0 r v = \rho r^3 g \quad (5)$$

where r_0 is the slurry concentration, and r is the particle size, which can be further deduced as follows in Formula (6):

$$v = \frac{\rho r^2 g}{6\pi r_0} \quad (6)$$

It can be seen from Formula (6) that the sedimentation velocity of microparticles in cemented slurry has a quadratic power relationship with their particle size. Therefore, the settling velocity of these particles in slurry will decrease greatly with a decrease in particle size. The particle size of fly ash and Portland cement generally ranges from 0.5 to 300 μm , and the fine aggregate particles can be suspended in slurry for as long as 1 to 2 h for the transportation process [65].

Initially, the mass percent of the solid in mixed slurry is as much as 60%–68% by adding normal cement in hydraulic slurry [16]. In order to further reduce the backfill cost and improve the properties of the cemented material during the transportation and activation stages, professional cementing agents suitable for underground coalmines are invented, and coal ash is introduced to replace certain parts of normal Portland cement [66,67]. Consequently, the mass concentration of the cemented backfill material is increased up to 70%–78%, and the modified material exhibits apparent pasty characteristics [39,68]. Nowadays, the mass percent of the solid in paste backfill material reaches as much as 76%–86%, as shown in Figure 12. The change in the mass percent of the solid in the filling material from year to year indicates that the filling slurry concentration needs to be determined by other conditions after the basic transportation requirements are met, and these engineering geological conditions are usually different for each mine.

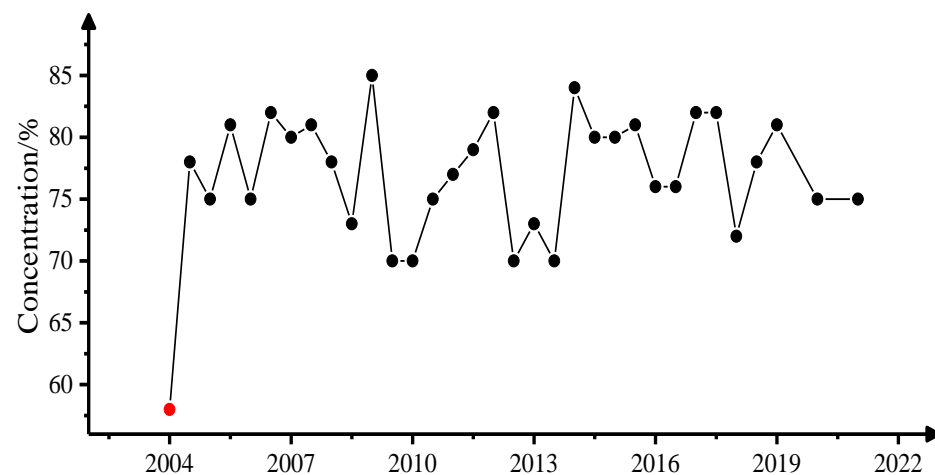


Figure 12. Variation trend in the concentration of the cemented filling slurry over the years. The red dots indicate that the concentration of the cemented filling slurry has not been reached since the previous time, while the black dots indicate that the concentration of cemented filling slurry has been reached later in time.

With an increase in the concentration, the flow theory of slurry also changes to structural flow from two-phase flow. As shown in Figure 13, the aggregate particles (gangue, gravel and sand) will be wrapped by the microparticles (cement and fly ash) and will not settle for a longer time. Consequently, the transportation distance of the mixed cemented filling slurry can be improved considerably, and the transportation mode is changed to structural flow (i.e., Bingham fluid) from two-phase flow.

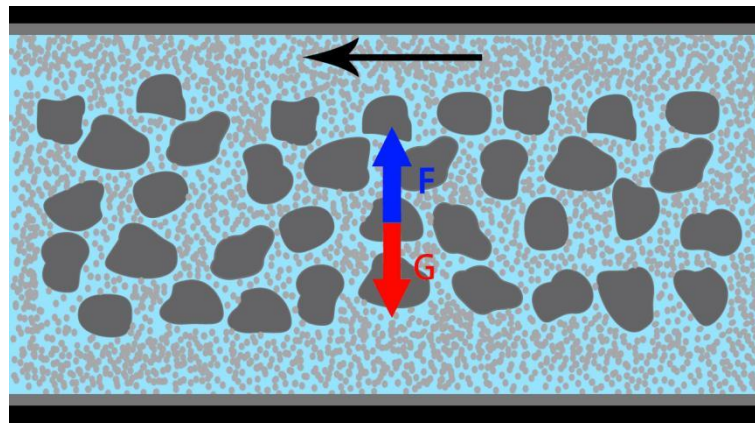


Figure 13. Aggregate stress in the structural flow of the transportation mode.

As for the Bingham fluid, there is an initial shear stress or yield stress in paste slurry, and the rheological curve is a straight line with a cut on the shear stress axis. Only when the shear stress exceeds this yield stress can suspension start to flow. The shear force and shear rate linearly increase, the slope of the line is the plastic viscosity coefficient, and the flow index is one. The rheological equation is

$$\tau = \tau_0 + \eta\dot{\gamma} \quad (7)$$

where τ is the shear stress; τ_0 is the yield stress; η is the viscosity coefficient; and $\dot{\gamma}$ is the shear rate [33].

The machines for the transportation of cemented backfilling material involve (1) wear-resistance pumps for providing force to drive the movement of the slurry; (2) monitors such as vortex flow meters, electromagnetic flow meters, mass flow meters, ultrasonic flow meters, isotopic densitometers, liquid level indicators, particle position indicators, electronic scales, etc., for the management of slurry transportation.

2.2.3. Activation of the Cemented Backfill Material

Compared with water–sand filling material, the bearing strength of cemented filling material is greatly improved and the overburden control effect is significantly improved due to the introduction of cement. The type and amount of cementing agents directly affect the performance of this kind of backfill material [69]. In underground coal mining, Portland cement, coal ash, gypsum and lime are commonly employed to bond aggregates of different particle sizes together through a hydration reaction to generate backfill masses with a certain strength. In tests, the curing time of the cemented paste mixture was determined, which was carried out in accordance with the standard using the Vicat apparatus [70,71]. In the tests, a measurement of the penetration depth of a steel needle with a diameter of 1 mm was taken under a specific weight of the moving part of the apparatus. The tests were completed when the steel needle was submerged to a depth of less than 3 mm [72].

Activation of Portland cement: Dry Portland cement appears as a powder, Portland cement clinker is a kind of multiminer aggregate and the main mineral composition is tricalcium silicate (C_3S), dicalcium silicate (C_2S), tricalcium aluminate (C_3A) and tetracalcium ferroaluminate (C_4AF) [45].

As shown in Table 1, the hydration reactions of mineral components in cement are as follows: The content of tricalcium silicate (C_3S) in cement clinker generally accounts for approximately 50%, sometimes up to 60% or more. Therefore, the hydration products of C_3S and the corresponding structure formed determine the performance of the cemented backfill mass, and the corresponding reaction is shown in Equation (8). The hydration rate of dicalcium silicate (C_2S) is very slow, which is approximately 1/20 that of tricalcium silicate, and its reaction is shown in Equation (9). The hydration reaction of tricalcium aluminate (C_3A) is rapid, and the composition and structure of its hydration products

are greatly affected by the concentration and temperature of calcium oxide and alumina in solution, and the reaction at room temperature is shown in Equation (10). When the liquid calcium oxide concentration reaches saturation, the reaction of tricalcium aluminate (C_3A) is shown in Equation (11), and the product C_4A_13 exists stably and increases in quantity under alkaline conditions, which is the main reason for the rapid solidification of cement. In the presence of gypsum and calcium oxide, tricalcium aluminate (C_3A) rapidly hydrates into C_4AH_{13} at the beginning, which then reacts with gypsum to form ettringite (AFt), as shown in Equation (12). When the gypsum is exhausted, the C_4AH_{13} formed by hydration of tricalcium aluminate (C_3A) can react with the ettringite previously formed (AFt) according to Equation (13) to form calcium sulphoaluminate hydrate (AFm). When the amount of gypsum added is very small, there may still be tricalcium aluminate (C_3A) unhydrated after all of the ettringite (AFt) has been converted to monosulphide calcium sulphoaluminate (AFm). In this case, a solid solution of C_4ASH_{12} and C_4AH_{13} is formed according to Equation (14). The hydration products of tricalcium aluminate (C_3A) are varied according to the gypsum content. The hydration reaction of tetracalcium ferroaluminate (C_4AF) and its products are very similar to those(that) of (C_3A), resulting in a solid solution of calcium sulphoaluminate hydrate (AFm) and calcium sulfur ferrate hydrate, as shown in Equation (15) [26,53,69,73], and the SEM profile of the different mineral components are shown in Figure 14.

Table 1. Mineral composition of ordinary Portland cement clinker in China [36].

Minerals	Chemical Formula	Content (%)
C_3S	$3CaO \cdot SiO_2$	54
C_2S	$2CaO \cdot SiO_2$	20
C_3A	$3CaO \cdot Al_2O_3$	7
C_4AF	$3CaO \cdot Al_2O_3 \cdot Fe_2O_3$	14
CSH	$CaSO_4 \cdot 2H_2O$	3.5

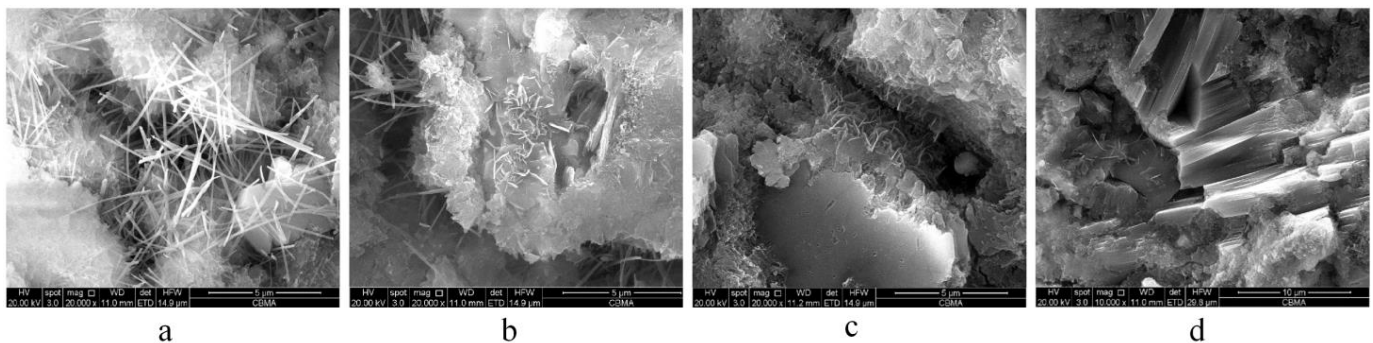
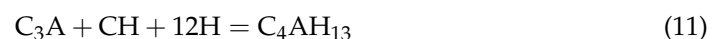
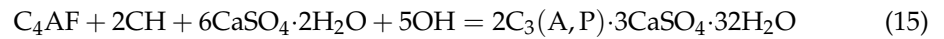
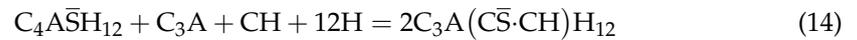


Figure 14. Hydration products of cement (SEM) [73]: (a) acicular AFt (3d); (b) flocculent CSH (3d); (c) stacked calcium hydroxide (7d); (d) rod AFt (7d).





Activation of coal ash: In order to reduce the filling cost, fly ash with a low cost and potential activity is added to the cementing material to replace part of the cement. The morphology effect (filling and dispersing) and pozzolanic effect of coal ash are the main reasons for its replacement of cement. (1) Morphology effect: Fine fly ash particles were distributed evenly in the filling slurry, which not only has the effect of filling the capillary porosity in the early hydration process of the cement material but can also effectively avoid the sticking together of the fine aggregate particles, scatter the flocculation structure of the hydration products, improve the uniformity of the slurry and hardening body, promote the hydration degree of the gelled material and, finally, improve the compactness and bearing strength of the solidified material [33,58]. (2) Pozzolanic activity effect: Fly ash particles contain active SiO_2 and Al_2O_3 , which can undergo a hydration reaction and generate gel hydration products. As fly ash is formed in a hot and flowing environment, its particles are mostly in the liquid glass phase. The proportion of Si-O, Al-O and Si-O-Al covalent bonds will affect the degree of polymerization of the silicate structure. The higher the number of covalent bonds, the greater the degree of polymerization, the lower the number of free vertices of fly ash particles and the more stable the structure will be. Therefore, the hydration of fly ash alone cannot produce gelation under normal circumstances, and the potential pozzolanic activity of fly ash can only be formed by artificial stimulation.

Physical activation of the pozzolanic activity of coal ash: The physical excitation to the pozzolanic activity of fly ash is mainly through destroying the surface mesh structure of fly ash particles by mechanical means, increasing the number of vitreous broken bonds, reducing the degree of polymerization and forming fly ash glass beads. As shown in Figure 15, the specific surface area of fly ash glass microbeads is large, the active components SiO_2 and Al_2O_3 are more easily dissolved and the hydration reaction is also faster. Qu et al. studied a method of reducing the amount of cementing material, in 2004, and concluded that the mechanical grinding of some fly ash can stimulate the chemical activity of the pozzolanic ash of pulverized coal [64]. In 2006, Lu et al. studied the influence of morphology and fineness on the activity of fly ash. The results showed that the activity of the spherical vitreous particles was the highest in fly ash, and the more vitreous the particles, the less porous the carbon particles and the higher the activity of the fly ash. The finer the fly ash, the better its quality and the higher its activity [69]. In 2018, Yin et al. conducted a physical grinding test on fly ash and found that after 20 min of physical grinding of the fly ash, the setting time of filling slurry could be significantly shortened, and the compressive strength of the solid filling materials could be improved [37].

Chemical activation of the pozzolanic activity of coal ash: The chemical excitation of the pozzolanic activity of fly ash is mainly achieved by adding a chemical activator to create a hydration reaction environment and by achieving interactions between useful chemical components in the chemical activator and active components of fly ash. There are three methods of chemical activation: first, the dense and smooth surface network structure of fly ash is destroyed by erosion; second, the activator can react with fly ash to produce hydration products with a certain strength and third, increase the calcium content of fly ash, that is, provide the substances required for the reaction. The commonly used activators are an alkaline activator, sulfate activator and chloride activator.

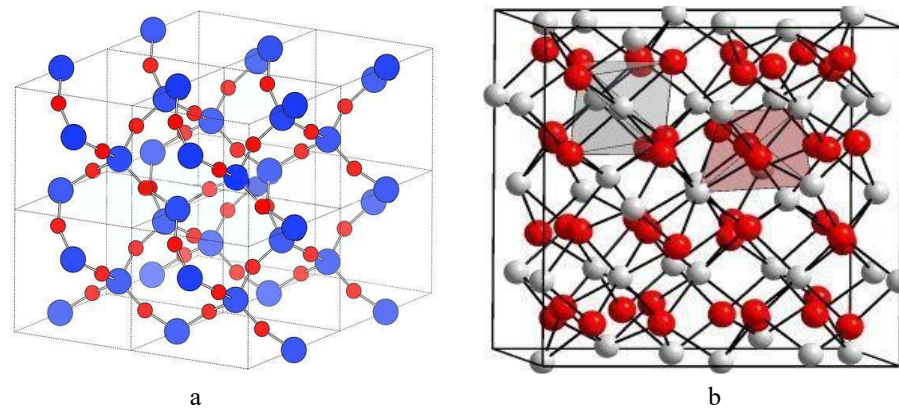
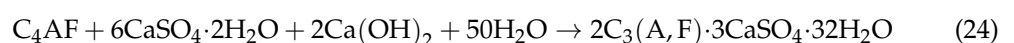
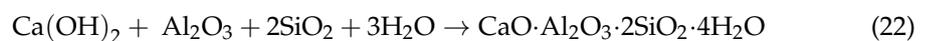
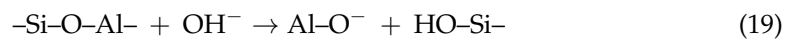
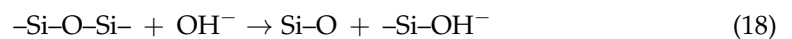
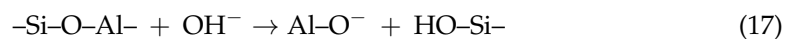
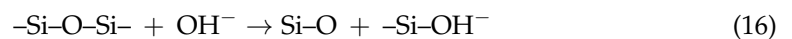


Figure 15. Molecular structure: (a) SiO₂ cell; (b) Al₂O₃ cell [37].

- (1) Alkaline chemical excitation: Fly ash is mainly composed of acid oxides, and its pH value is less than seven, showing weak acidity. SiO₂ is an acidic oxide, Al₂O₃ is an amphoteric oxide; they can react with OH[−] in alkaline aqueous solution so that the Si-O-Si bond, Al-O-Al bond and Si-O-Al bond are broken. After the stable vitreous networks are depolymerized, the active ingredients are in a free state, and unsaturated chemical bonds with high activity are formed. A chemical reaction occurs after mixing with cement and lime to form carburized body substances, such as calcium silicate hydrate (C-S-H), calcium aluminate hydrate (C-A-H), calcium silicate aluminate hydrate (C-A-S-H) and ettringite (Aft). The hydration products are cross-connected on the surface of fly ash glass beads to improve the mechanical strength of cemented filling materials after solidification.

Considering the acid-based nature of fly ash and the actual excitation cost, alkaline excitation is considered to be the most widely used and effective excitation method. Alkaline activators are mainly Ca(OH)₂ and NaOH, which have been studied by a large number of scholars. The reaction mechanism of the alkaline activation of the pozzolanic activity of fly ash is shown in Equations (16) and (17). Equations (18) and (19) will occur if there is Na⁺ or Ca²⁺ in the solution. The main hydration Equations (20)–(24) are shown in the following [53].



In 2008, Zhao et al. studied the products and structures of fly-ash-based cemented backfill materials after a hydration reaction of 4 h, 8 h, 12 h, 16 h, 20 h, 1 d, 3 d and 7 d using a scanning electron microscope and X-ray test. The results showed that ettringite was the main product of the hydration reaction, and its microstructure was fine-needle. Ettringite was evenly distributed on the surface of the aggregate particles, forming a “thorn ball” shape with a dense structure. Acicular materials grew reflectively and interweaved to form a spatial network structure, and the cement structure between the aggregate and matrix was stable [45]. In 2018, Yin Bo et al. constructed a reaction process and hydration product formation mechanism model of alkali-excited low-calcium fly ash and believed that the effect of alkali excitation on low-calcium fly ash was mainly manifested on the particle surface, and the surface modification promoted the particles to undergo four stages of change: dissolution, depolymerization, polycondensation gel and diffusion. The hydration process of filling materials is divided into three stages: dissolution, cement-fly ash hydration and structure formation and development. The results showed that with the extension of the hydration time, the hydration products, such as $\text{Ca}(\text{OH})_2$, C-S-H and AFt, continued to increase, and the filling material matrix was filled and consolidated by the hydration products, resulting in a reduced porosity and increased compactness [37], as shown in Figure 16.

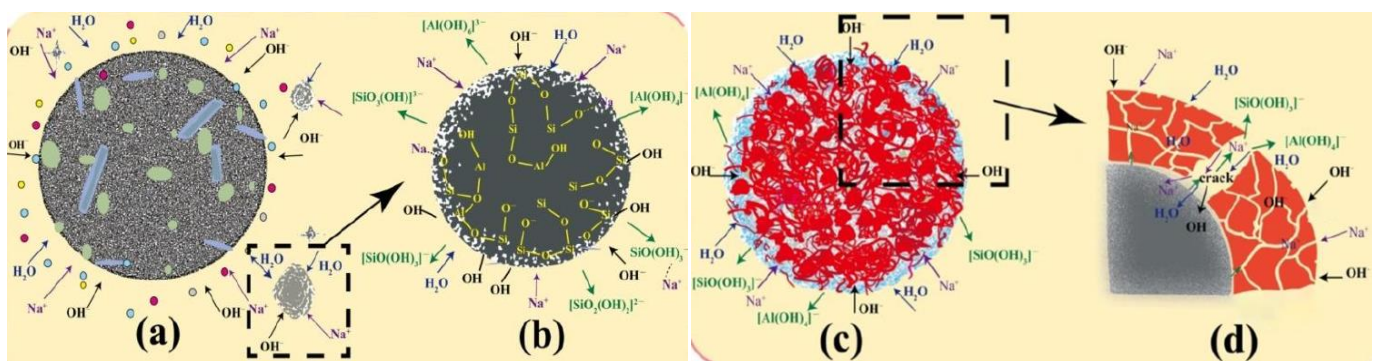
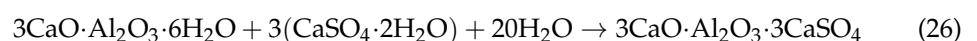
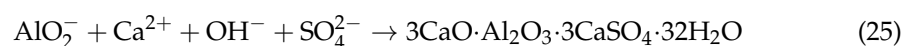


Figure 16. Reaction process and hydration product formation mechanism of low-calcium fly ash stimulated by alkali [37]: (a) dissolution stage; (b) depolymerization stage; (c) polycondensation and polymer gel stage; (d) diffusion stage.

- (2) Sulfate chemical excitation: The activated Al_2O_3 in fly ash reacts with $\text{Ca}(\text{OH})_2$ released by the hydration of cement material and SO_4^{2-} ions released by the dissolution of gypsum to generate ettringite and produce a gel phenomenon, which is called sulfate excitation of fly ash activity. When CaO , $\text{Ca}(\text{OH})_2$ and other “calcium supplement” substances are added to the solution, the solution will contain a large amount of OH^- . The potential (Al_2O_3) active substance in fly ash is firstly reacted with OH^- to form AlO_2^- and then reacts with Ca^{2+} and SO_4^{2-} to generate ettringite (AFt) with a certain gelation. The reactions are shown in Equations (25) and (26). The common sulfate activators are Na_2SO_4 , K_2SO_4 and CaSO_4 . For example, Na_2SO_4 is easily soluble in water and can react with $\text{Ca}(\text{OH})_2$ in solution and produce relatively dispersed CaSO_4 , which more easily produces calcium–vanadate than gypsum. Na_2SO_4 can also react with $\text{Ca}(\text{OH})_2$ in the solution to form NaOH , which increases the alkalinity of the solution. So, the excitation of Na_2SO_4 is actually a double excitation of a strong base and sulfate.



In 2021, Zhao et al. studied the influence of desulfurized gypsum content on the strength of cemented filling mass and found that the appropriate dosage of desulfurized gypsum should be controlled at 5%. The addition of desulfurized gypsum introduced a large amount of SO_4^{2-} into the solution and significantly improved the dissolution rate of fly ash particles. Consequently, the surface of the fly ash particles was rough and accompanied by pits and other products, thus effectively stimulating the activity of fly ash and releasing a large amount of active silicon and aluminum, which finally combined with the external Ca^{2+} , SO_4^{2-} and OH^- , forming hydration products such as C-S-H, C-A-H and AFt. These amorphous gels and pin-stick AFt crystals are inserted and wrapped in the filling mass, which reduces the porosity of the material, optimizes the void structure and improves the overall connection [73], as shown in Figure 17.

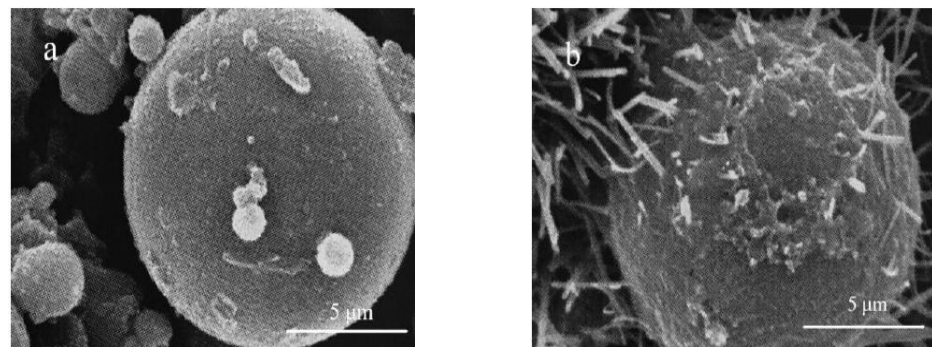


Figure 17. SEM images of fly ash particles [74]: (a) without desulfurized gypsum; (b) with desulfurized gypsum.

Chlorine salt chemical excitation: The excitation mechanism of chloride salt on fly ash is mainly to provide a large amount of Cl^- for the solution. Due to the strong diffusion ability of Cl^- , it can fully contact with fly ash. Common chlorine activators include CaCl_2 and NaCl . CaCl_2 is a soluble salt, and Ca^{2+} and Cl^- can be evenly dispersed in the solution. With the increase in the curing age, Ca^{2+} is gradually consumed in the hydration reaction. The Ca^{2+} in CaCl_2 plays the role of a “calcium supplement” for the filling material and combines with the Cl^- passing through the hydration film to generate more calcium chloroaluminate hydrate and calcium silicate hydrate. The reaction is shown in Equation (27). NaCl mainly provides Na^+ and Cl^- , and Cl^- can react with Al_2O_3 and CaO to produce calcium chloroaluminate hydrate. Na^+ combines with OH^- in the solution to form a strong alkali NaOH , which provides an alkaline environment for the hydration of fly ash and increases its ability to disintegrate vitreous structure, as shown in Equation (28).



In 2011, Ren et al. studied the influence of alkaline activator–sodium hydroxide, chloride activator–sodium chloride and sulfate activator–sodium sulfate on the pozzolanic activity of fly ash. The results showed that the alkaline activator, chloride activator and sulfate activator all promoted the pozzolanic activity of fly ash. In terms of the effect, the alkaline activators and sulfate activators were obvious, and the chlorine activators were relatively weak [68]. In 2017, Yu et al. conducted a chloride salt excitation test, and the experimental results showed that the chloride activator and sulfate activator had the same effect on the compressive strength of the mortar block, and the compressive strength of the mortar block increased with the increase in the content of the activator. When the NaCl content was 1.5%, its compressive strength at 3 d, 7 d and 28 d was 14.51 MPa, 24.75 MPa and 39.74 MPa, respectively. When the CaCl_2 content was 1.5%, the compressive strength

at 3 d, 7 d and 28 d was 14.24 MPa, 25.87 MPa and 40.36 MPa, respectively [53], as shown in Figure 18.

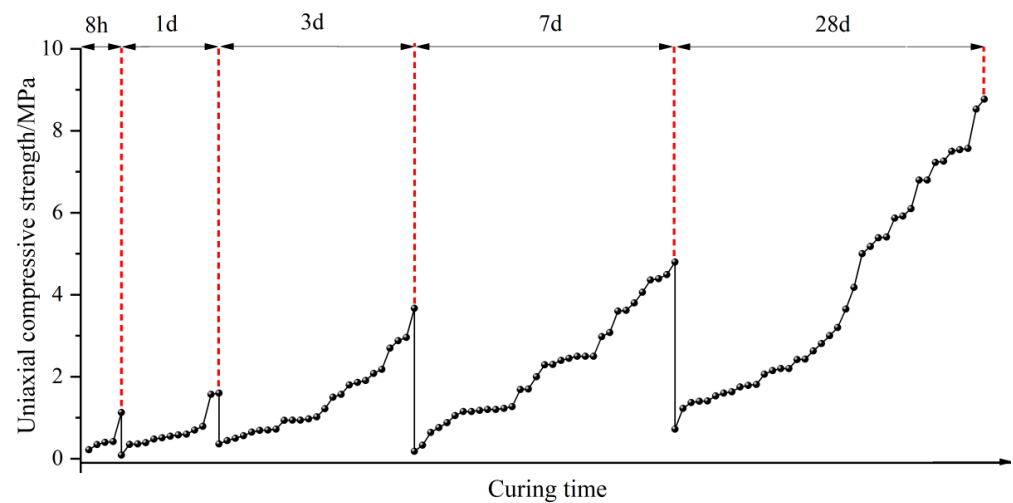


Figure 18. Strength of cemented backfill at different curing ages.

2.2.4. Time Needed to Fill the Post-Mining Space with Cemented Backfill Material

Compared with hydraulic backfill material, the time needed for filling the goaf with cemented filling material is greatly shortened. Due to the addition of fine aggregate, such as fly ash and cement, the slurry concentration of cemented filling material is greatly increased. The high concentration of cemented filling slurry is not easy to isolate and block during transportation, which makes the transportation of the filling material from the ground to the goaf more time saving and efficient. The result is that the gob can be filled more quickly. In addition, after the cemented filling material is filled in the goaf, the water in the slurry does not need to be removed from the goaf, and the time-consuming water filtration process is canceled, further shortening the time for the cemented filling material to fill the goaf. Moreover, when the goaf is filled with cemented filling material, the goaf can be completely filled.

2.2.5. Evaluation of the Cemented Backfill Material

Advantages: Firstly, the cemented backfill material can be transported more efficiently. The liquid cemented slurry can remain in a stable state without segregation for a long time. Thus, it can be transported through a pipeline for a greater distance in large quantities without blocking compared with hydraulic backfill material. Secondly, the mechanical strength of the solid cemented backfill material is larger due to the fact that particles are cemented together by the chemical reaction between water and the cementing agent. Last, but not least, all water added in the preparation stage can be stored in the fills and become one part of the bearing structure of the final solidified mass, and there is no redundant water bleeding out of the gob anymore. As a consequence, all structures and equipment for water drainage and recycling are not needed, and the efficiency and economical reasonability can be improved considerably.

Disadvantages: There is a high level of investment because of the large cement agent consumption. Several additives are always applied collectively to achieve the desired performance of the cemented backfill material due to the fact that each additive commonly has a significant effect only on a certain characteristic of the target material; on the other hand, the characteristics have limited influence. Thus, a large quantity of the mixed additives is added to the cemented backfill material, which not only optimizes the performance of the backfill material but also increases the cost considerably. For example, the unconfined compressive strength of the solidified material modified by the aforementioned additives reached 0.4 MPa, 0.83 MPa and 1.02 MPa after 8 h, 1 day and 3 days of the curing process

with a slurry concentration of 81%, cementing agents of $80 \text{ kg}\cdot\text{m}^{-3}$ and fine aggregate (i.e., fly ash) of $400 \text{ kg}\cdot\text{m}^{-3}$. While the corresponding strength of the solidified material with the same components decreased to 0 MPa (8 h), 0.1 MPa (1 day) and 0.29 MPa (3 days) when the modifying additives were not employed [52,66,67].

2.3. High-Water Backfill Material

High-water backfill mining is the third backfill mining method that is largely employed in Chinese underground coal mining. The solid components of the high-water backfill material can be divided into two parts, which are mixed with water to make Slurry A and Slurry B and separately transported to an underground backfilling station and mixed [75]. Once the mixed grout is backfilled into the gob, Slurry A and Slurry B will react and solidify quickly, supporting the overlying strata, as shown in Figure 19. A significant improvement in the high-water backfill material compared with the cemented one is that the flow performance is greatly improved by significantly reducing the concentration of the slurry during transportation [76]. Most importantly, once Slurry A and Slurry B are mixed in the underground gob, the large amount of water added during transportation will take part in the reaction between Slurry A and Slurry B and finally become one part of the solidified body and remain in the gob rather than flow out of the gob as excess water. It can be said that the invention of high-water materials completely solved the problem of the long-distance transportation of underground backfilling materials.

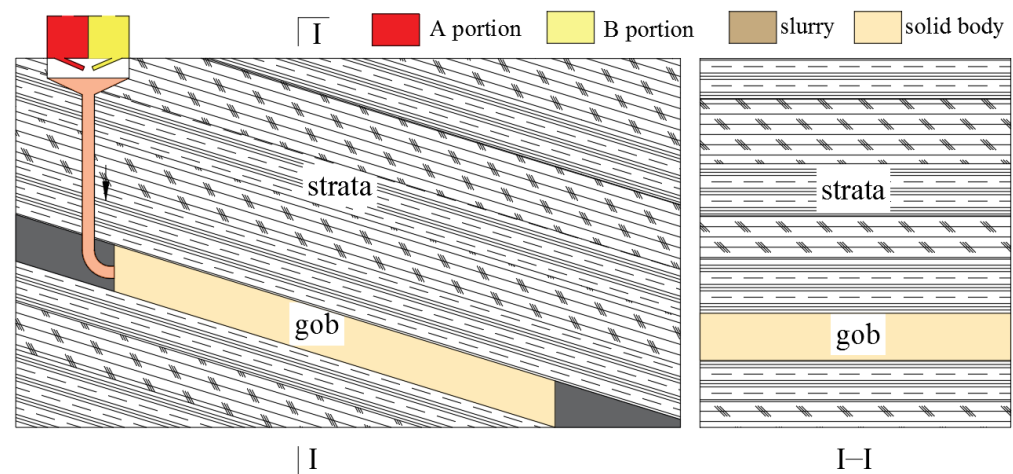


Figure 19. High-water backfill mining system.

2.3.1. Preparation of High-Water Backfill Material

The solid components of high-water backfill material are mainly divided into two parts; one part consists of material A and its auxiliary material AA, and the other part consists of material B and its auxiliary material BB, and the proportion of different raw materials in each part are illustrated in Figure 20. Data statistics: Sulphate aluminum cement, bauxite clinker and fly ash are always employed as the main components of material A, providing the necessary raw materials for the final hydration reaction; a retarder, suspending agent and dispersing agent are often used as the main components of material AA, allowing for material A to remain stable solely in slurry without subsiding and solidifying for a long time. Lime, gypsum and cement are always selected as the main components of material B, preparing the necessary Ca^{2+} and SO_4^{2-} for the final hydration reaction; an accelerator, suspending agent and early strength agent are often chosen as the main components of material BB, ensuring that the hydration reaction can take place as soon as the desired amount of Slurry A and Slurry B are mixed. The solidified mass can achieve a mechanical strength as high as possible at the early solidifying stage to control the potential subsidence of the roof strata over the goaf.

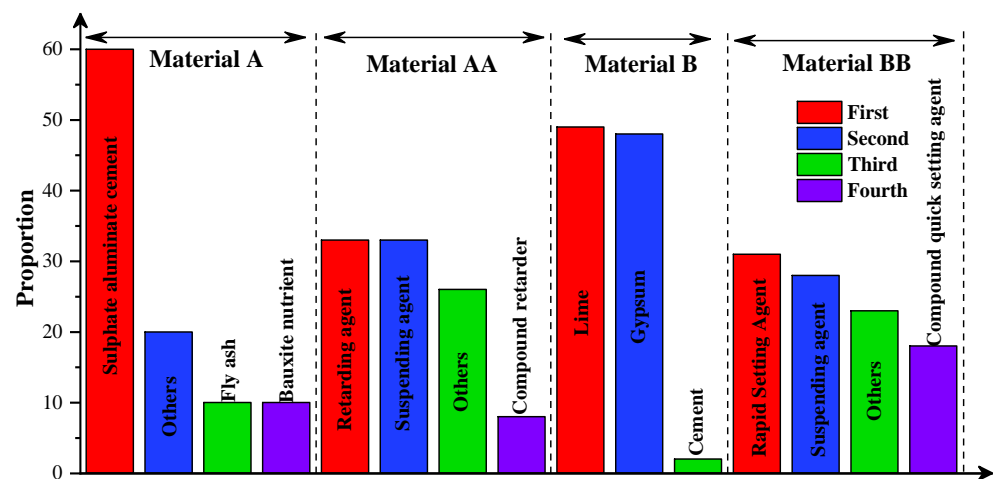


Figure 20. Percentages of the different materials high-water backfill material.

At present, the pulping process of high-water materials can be controlled by PLC (programmable logic controller of a digital operation electronic system), as shown in Figure 21, which is fully automated. The system has independent feeding, water and material weighing, mixing, auxiliary material supply and an unloading system. Each process is coordinated in time and completed independently in space. This not only ensures the accuracy of the material ratio but also makes it easy to observe the location of the problem and fix it in time, and the system works efficiently.

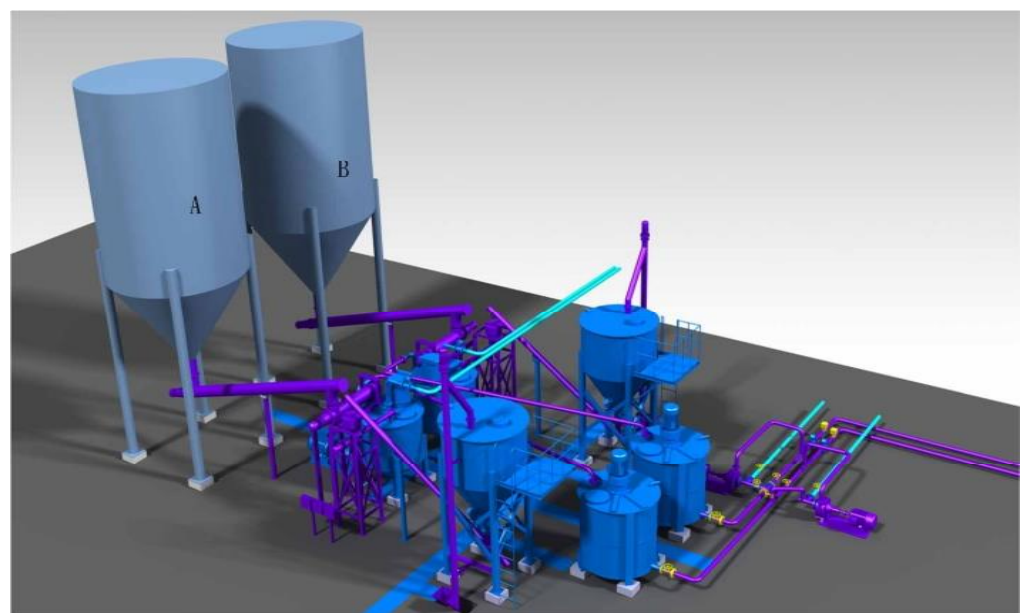


Figure 21. Automatic pulping system of the high-water material.

2.3.2. Transportation of the High-Water Backfill Material

As mentioned above, cemented backfill material exhibits structural flow characteristics by increasing the slurry concentration during transportation, and the backfill slurry can be pumped for a longer distance without segregation compared with the original water-sand backfill slurry. The high concentration, however, inevitably enlarges the frictional resistance between the slurry and the pipeline. Consequently, the requirements for the pumping equipment and transportation cost are increased [77]. In order to improve the backfilling slurry's pumpability and reduce the flow resistance of the slurry in the pipeline, the improved high-water backfill material is transported underground smoothly

by reducing the slurry's concentration via adding a large amount of water, rather than the cemented backfill material, the pumpability of which is improved by increasing the slurry concentration by reducing the amount of water added [78]. Firstly, two kinds of powdery solid aggregates are mixed with water on the grounds to produce Slurry A and Slurry B. The volume ratio of the water in Slurry A and Slurry B can reach much more than 90%. Consequently, the powdery solid aggregate can suspend in the slurry and will not subside for a long time, and the transportation distance and efficiency can be significantly increased; at the same time, the pumping pressure and transportation costs are reduced [26].

In 2010, Feng et al. studied the change rule of the flow performance of a single slurry of high-water material over time and found that the slurry did not solidify within 30~40 h and the flow performance was good. Such grout can be considered a Newtonian fluid and is ideal for long-distance transport in pipelines [79]. In 2011, Feng et al. further studied the changing law of the flow performance of the mixed grout of high-water materials over time and found that when the grout approached the condensation time, the viscosity curve had an inflection point and then rose rapidly over a short time, and the grout lost its fluidity and became a non-Newtonian fluid [77]. In 2012, Jiang et al. studied the influence of the water content on the viscosity of high-water material's mixed grout at an initial setting and found that the viscosity value of the grout at an initial setting time of 30 min was approximately 1400 mPa·s and that at 60 min was approximately 1070 mPa·s. They believe that when conveying slurry through a pipeline, if the initial setting time is short, it is easy to block the pipeline at the setting time [80]. In 2013, Jiang et al. studied the influence of a suspending agent and retarder on the flow performance of Slurry A of high-water material and found that when the water–solid ratio was three, the volume changed and the bleeding rate of Slurry A decreased significantly only when the suspending agent content reached 4%. When the water–solid ratio was two, the setting time for Slurry A increased gradually with the increase in the retarder dosage. Given that the setting time of Slurry A is usually within 24 h, the amount of retarder is capped at 1.8% [81]. In 2014, Xie et al. studied the influence of temperature on the initial setting time of high-water material mixed grout and found that the initial setting time of the grout decreased slowly with the increase in the temperature when the temperature was lower. When the temperature was higher than 20 °C, the initial setting time decreased rapidly with the increase in the temperature [82]. In 2014, Li et al. studied the characteristics of equipment selection in the backfilling process of high-water materials. For the conveying pump, a piston pump with the characteristics of large conveying pressure, accurate conveying capacity and stable system operation should be selected as the power source of the slurry transportation. For the conveying lines, seamless steel pipes should be selected to ensure sufficient strength to prevent the pipes from bursting. The flow of the slurry will drive the pipeline to vibrate violently, so the pipeline joint should be connected with a flange to prevent slurry leakage. The phenomenon of the large resistance caused by right-angle turning and pipe diameter change should also be minimized or avoided. For a mixed slurry system, it should be composed of three parts: tee, mixing pipe and spiral sheet. In order to ensure sufficient mixing of the slurry, the length of the mixing pipe should be no less than 60 m. As the mixing device needs to be moved along with the movement of the backfilling working face, the mixing pipe should not be too heavy, and it is usually made of 5 m long seamless steel pipes with flanges [83]. In 2015, Lu et al. conducted field transportation tests on high-water grout and found that the flow rate of grout in the pipeline should be kept between 2.2 m/s and 3.2 m/s. If the flow rate is too fast, this easily increases the transportation resistance, leading to a large loss in the pipeline pressure and pipe lug damage. If the flow rate is too slow, the slurry easily solidifies in the pipeline or is deposited at the bottom of the pipe [84]. In 2017, Zhou et al. found that the gelling time of mixed grout could be shortened to 10 min without reducing the setting time of the single grout by accelerating the hydration rate of anhydrous calcium sulphoaluminate in sulphoaluminate cement [85]. In 2018, Sun et al. studied the influence of the stirring time on the bleeding rate of high-water grout and found that an increase in the stirring time can increase the reaction time between substances in

the grout, make the reaction more uniform and effectively reduce the bleeding rate of the grout in the transportation process [86].

2.3.3. Activation of the High-Water Backfill Material

After the high-water content in Slurry A and Slurry B is fully mixed, a hydration reaction will occur, and hydration products, such as ettringite and calcium silicate hydrate gel, will be generated. Hydration products are the main reason for the bearing strength of high-water slurry after curing [82]. The hydration reactions are as follows (Figure 22).

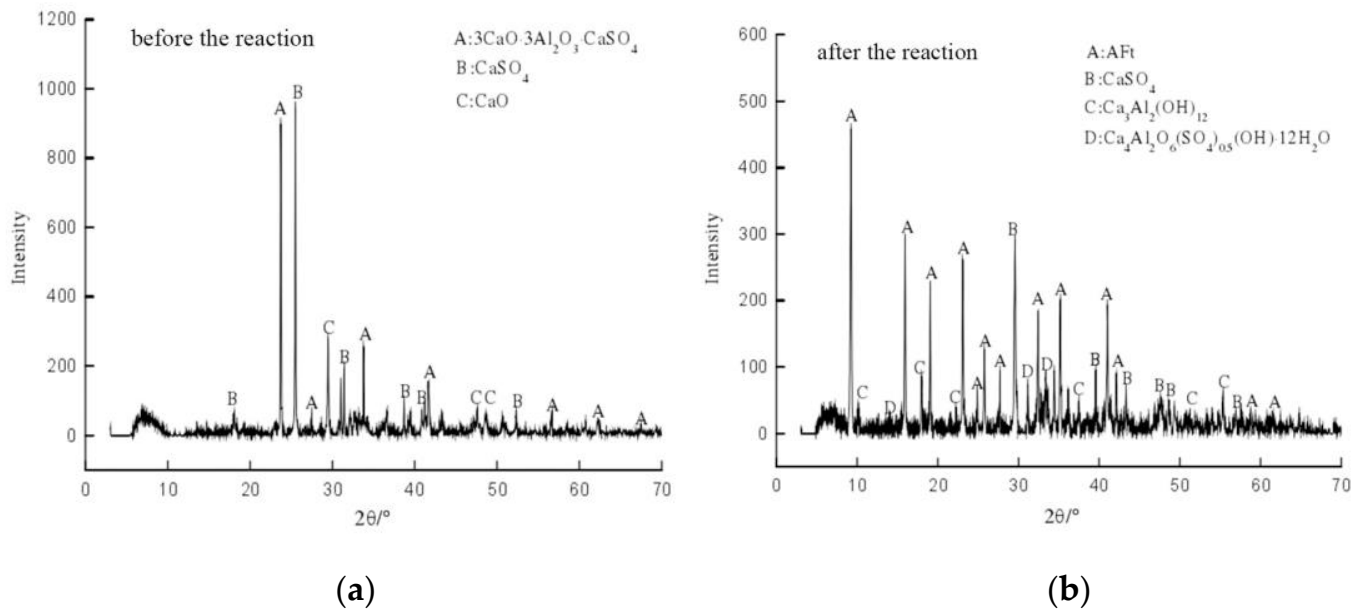
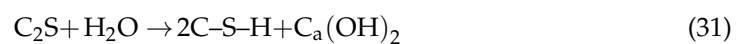


Figure 22. XRD pattern of high-water filling material before and after the hydration reaction, (a) before the reaction; (b) after the reaction [27].

Firstly, under the action of gypsum ($\overline{C}\overline{S}H_2$), lime (CaO) and other admixtures, the reaction of anhydrous calcium sulfate ($\overline{C}_4\overline{A}_3\overline{S}$) in sulfoaluminate cement clinker takes place according to Equations (29) and (30), rapidly forming a large number of columnar ettringite crystals ($\overline{C}_3\overline{A}\cdot 3\overline{C}\overline{S}\cdot H_{32}$). After, the disalcium silicate ($\overline{C}_2\overline{S}$) in Slurry A will also slowly undergo a hydration reaction with water, according to Equation (31), to form calcium silicate hydrate gel (C-S-H), which contributes greatly to the later strength of the solidified high-water backfills. In addition, the generated calcium hydroxide ($Ca(OH)_2$) can continue to participate in the reaction (29) to form ettringite crystals. The aluminum gel (AH_3) and silica gel (C-S-H), formed by reactions in Equations (29) and (31), and the unbound water in the high-water slurry will fill the spatial network framework formed by ettringite crystals. Gel can increase the density of the structure, improve the water retention performance of the whole hardened body and further improve the strength of the filling body. The unbound water in the high-water slurry fills in the voids of the network structure and is divided into droplets of various sizes and shapes. Due to the action of the capillary force and adsorption effect, these droplets have a certain “bonding” and “filling” effect between the solid phase, which further enhances the strength performance of the high-water filling body [80,81].



In 2018, Sun et al. conducted scanning electron microscopy (SEM) tests on the microstructure of high-water filling materials after curing, as shown in Figure 23, and found that when the curing time was 1 day, the main shape of ettringite was cylindrical with a length of 6–10 μm . At this time, the ettringite distribution was relatively loose, and there were some flakes of calcium sulfoaluminate in the ettringite gaps. When the curing time was 3 days, the ettringite was a mixture of needle-like and columnar shapes, with a needle-like length of 2–4 μm and columnar length of 6–10 μm . The density of the ettringite increased, and the content of the calcium sulphoaluminate decreased. When the curing time was 7 days, the morphology of the ettringite changed little, and it was mainly acicular, and part of the aluminum hydroxide existed in the ettringite [86], as shown in Figure 23.

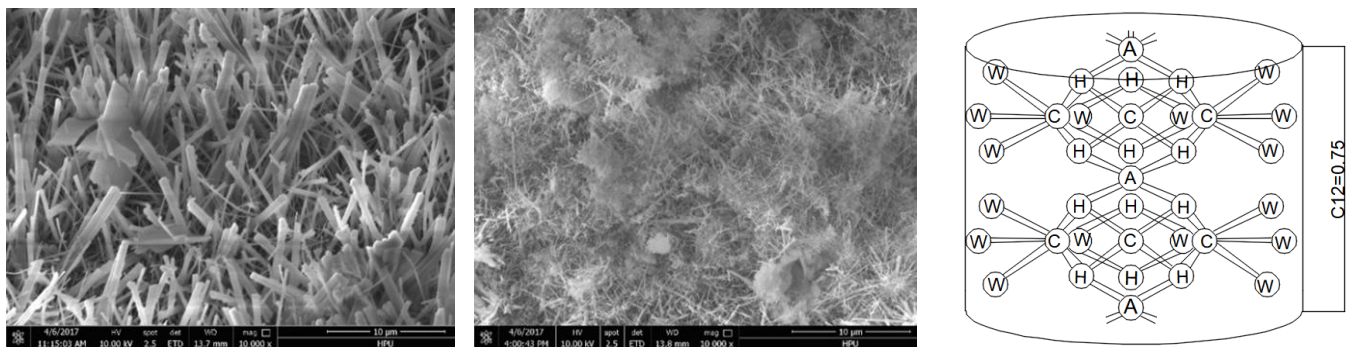


Figure 23. Microstructural diagram of high-water material after a hydration reaction (1 d, 3 d, and 7 d). Molecular structure of ettringite in high-water consolidation (A-Al, C-Ca, H-OH, and W-H₂O) [86].

Ettringite crystals are composed of six calcium atoms arranged in an oriented manner, and their basic structure is columnar. Each calcium atom can have four water molecules attached to it. On the outer side, parallel to the vertical axis, there are four grooves, three of which each combine one sulfate ion and two water molecules. Therefore, a total of 32 water molecules are required for the formation of complete ettringite cells, accounting for 81.16% of the total volume of ettringite crystals.

The amount of water crystal in ettringite is related to the ambient humidity. Among the 32 water molecules consolidated on ettringite crystals, 24 are bound water and 8 are crystallized water. The 24 bound water molecules can be divided into two parts: primary vertex water and secondary vertex water, according to the different bond lengths with calcium atoms. The former is more firmly bound and not easy to lose, and the latter bond is relatively weak and easy to lose. Eight crystals are in the grooves parallel to the longitudinal axis laterally, where they are weakly bound to calcium atoms and are easily lost [79].

According to statistics, the uniaxial compressive strength of high-water filling materials in China's coal mines can reach 1.46 MPa within 8 h after curing, 1.81 MPa within 1 d, 4.26 MPa within 3 d, 7.20 MPa within 7 d and 11.7 MPa within 28 d. Generally speaking, when high-water materials are used for dense filling in the goaf, the uniaxial compressive strength of 2–3 MPa can satisfy the purpose of controlling the overburden movement. When the goaf is partially filled with high-water materials, its strength is highly required, and the specific value is related to the size of the filling structure, as shown in Figure 24.

2.3.4. Time Needed to Fill the Post-Mining Space with High-Water Backfill Material

Compared with cemented filling material, the time needed to fill the goaf with high-water backfill material is further shortened. Since the concentration of high-water backfill material is very low during transportation, there is almost no need to worry about the influence of the solute precipitation and plugging in the slurry. Therefore, the goaf space is more easily filled. In addition, like cemented filling material, after high-water backfill material is filled in the goaf, the water in the slurry will not be removed from the goaf, saving a lot of time in the process of water filtration and water collection. At present, high-water filling material has the shortest time required to fill the goaf.

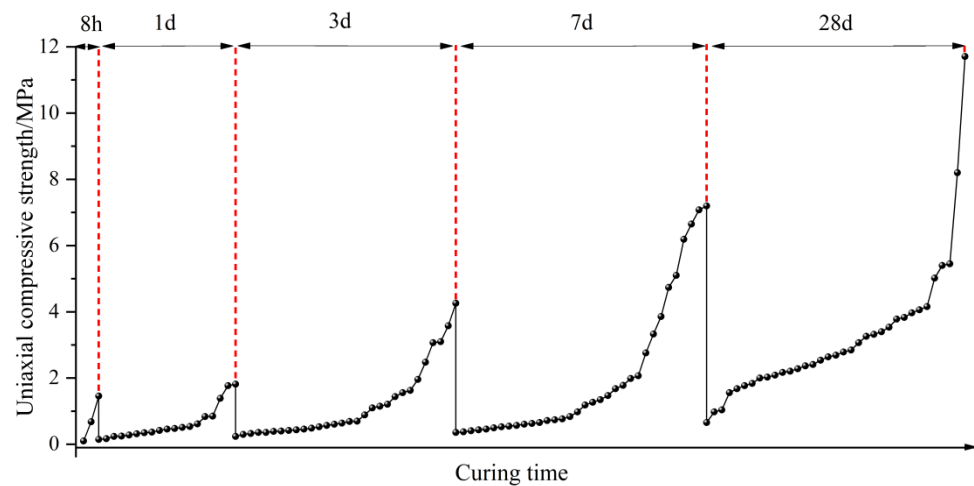


Figure 24. Uniaxial compressive strength of high-water filling material at different curing ages [22,78,80,81,84–87].

2.3.5. Evaluation of the High-Water Backfill Material

Advantages: Firstly, the transportation efficiency of high-water filling material is further improved compared with that of cemented filling material. Due to the low concentration resulting from the high-water content, there is less friction between the grout and the pipeline to overcome when the high-water grout is transported from the ground to the underground goaf. The result is long-distance transportation with a low pumping pressure. In addition, the high-water filling material is pumped separately by Slurry A and Slurry B. Each slurry can maintain a good flow performance for a long time before mixing, ensuring that segregation and even consolidation of the plugging phenomenon do not occur during long-distance transportation. Secondly, high-water filling materials have strong adaptability to different filling conditions. The consolidation strength of the high-water filling material is provided by the hydration product generated after the mixture of the A and B contents. Therefore, there are few factors affecting the consolidation strength of high-water filling materials, and it is easy to achieve quantitative control. The result is that the consolidation time and consolidation strength of high-water filling materials can be precisely controlled according to different underground bearing requirements, and the control effect on the stability of the overburden strata can be achieved under different working conditions [81].

Disadvantages: First of all, backfilling with high-water materials consumes a large amount of water resources. No matter the transportation in pipes or the acquiring of bearing capacity in the goaf space, water with a volume ratio of up to 90% is needed. This is unacceptable in mining areas that are already water scarce, such as the arid regions of Northwest China. Secondly, the field operation of high-water backfilling is difficult. Because the consolidation time and consolidation strength of high-water backfilling materials are highly sensitive to the ratio of components, in high-water filling construction, all possible impacts from other mining operations, such as coal mining, ventilation and transportation, must be predicted in advance, and precise responses have to be made as soon as possible, which is more difficult to achieve in a busy and complicated mining field. Finally, the stability of high-water consolidation is poor. Because the consolidation body of high-water filling material contains a large amount of water, especially weak bound water, it is easy to run off after the long-term effect of ground temperature (ground temperature increases with depth), which leads to the structural damage of the high-water filling body, reduction or even loss of the bearing strength and loss of support for the rock strata at the top of the goaf.

3. Waterless Backfill Material

3.1. Gangue Backfilling Material

Gangue backfill mining is the fourth backfill mining method that is largely employed in Chinese underground coal mining. The main component of gangue backfill materials is the waste rock that is separated from the mined coal [59]. Firstly, the gangue piled on the ground will be broken into a required lumpiness and then transported to the underground goaf through a preprepared channel [88–90]. In the goaf, gangue will be compacted to a certain extent and then the goaf is filled to support the rock strata above the goaf, as shown in Figure 25.

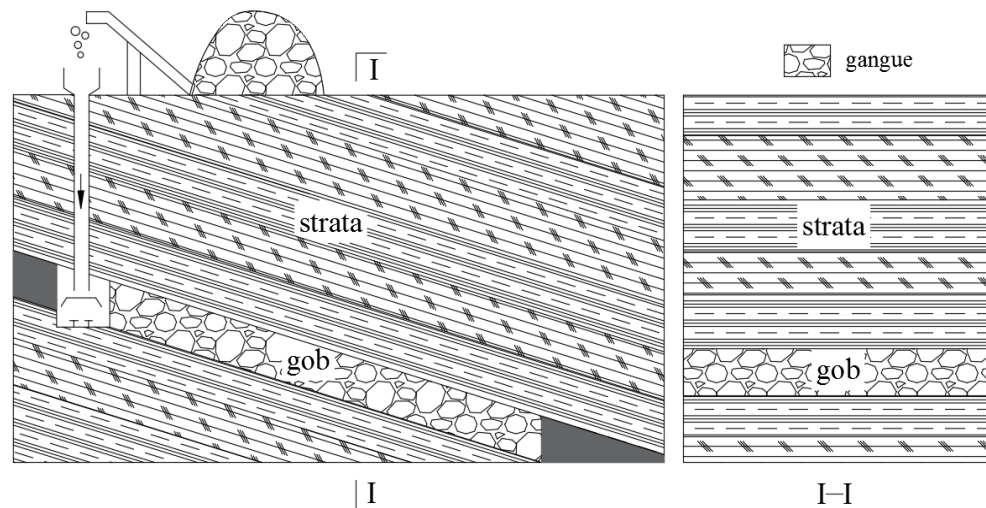


Figure 25. Gangue backfill mining system.

3.1.1. Preparation of the Gangue Backfill Material

As mentioned in Section 2.2.1, gangue is an associated product in coal mining, accounting for approximately 30% of the entire coal production in weight, and the original gangue is always large in size and poor in grading. In order to make the gangue easily transportable and achieve a greater compactness after backfilling into the goaf, the original gangue should be broken into an appropriate lumpiness [91]. Of course, compared with cemented backfilling, a gangue backfilling system has fewer requirements regarding the gangue grain size and grading. According to statistics, in China’s gangue filling practice, gangue is usually broken into seven particle size groups, ≤ 5 mm, 5~10 mm, 10~20 mm, 20~30 mm, 30~40 mm, 40~50 mm and ≥ 50 mm, as provided in Table 2.

Table 2. Grain size grading of gangue in gangue backfilling.

VII (mm)	IV (mm)	XII (mm)	IX (mm)	VI (mm)	III (mm)	II (mm)	I (mm)	Reference
150~125	100~125	75~100	50~75	25~50	10~25	5~10	2.5~5	[92]
		>25	20~25	15~20	10~15	5~10	≤ 5	[93]
		25~30	20~25	15~20	10~15	5~10	0~5	[94]
		25~31.5	20~25	16~20	10~16	5~10	0~5	[95]
				30~40	20~30	10~20	0~10	[96]
			16~20	9.5~16	5~9.5	2.36~5	≤ 2.36	[97]
40~50	31.5~40	25~31.5	20~25	16~20	10~16	5~10	0~5	[98]
				30~40	20~30	10~20	0~10	[99]
			40~50	30~40	20~30	10~20	0~10	[100]

3.1.2. Transportation of the Gangue Backfilling Material

The biggest difference between the transportation of gangue filling materials and that of previous filling materials is that water is no longer used as the floating medium

of solid materials. This means that gangue filling materials can rely on their own gravity as the power for vertical movement, while horizontal transportation requires additional mechanical assistance [59]. In 2012, Ju et al. believed that the vertical dumping system of gangue should include the ground feeding control part, the gangue vertical passage part, the material buffer part and the material storage part, as shown in Figure 26a. Moreover, he discovered a phenomenon where gangue would eventually realize uniform motion due to the action of air resistance in the process of vertical descent by fluent numerical simulation. In 2014, Kang et al. further proposed the method of the transverse transportation of gangue in the goaf, that is, hanging a scraper conveyor below the rear roof beam of the hydraulic support. When the gangue is running on the scraper conveyor, it can be transported to any designated place in the goaf by controlling the opening/closing of the leak hole on the diaphragm, as shown in Figure 26b. In 2018, Li et al. further studied the movement law of gangue with eight particle sizes (5, 10, 15, 20, 25, 30, 40 and 50 mm) in vertical pipelines, and the results were as follows [99].

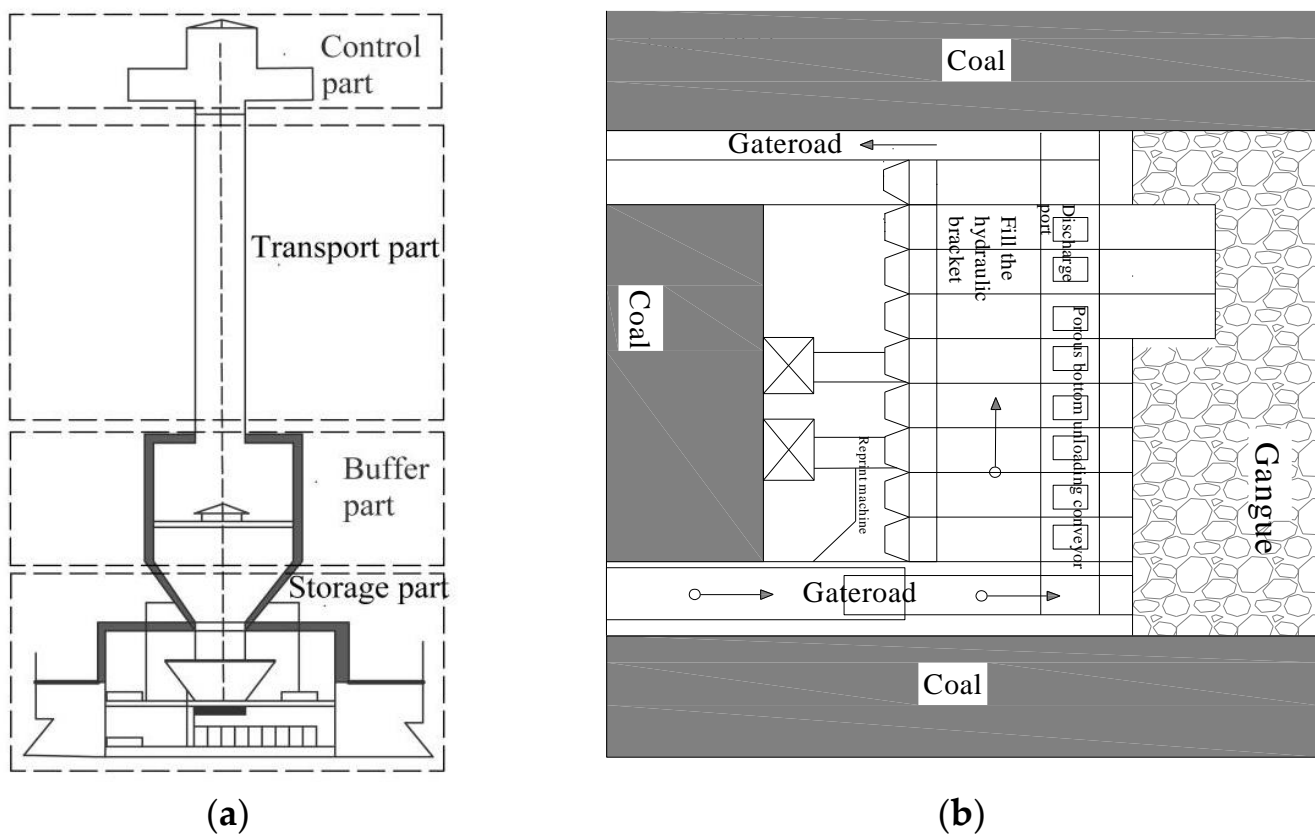


Figure 26. Vertical and horizontal transport systems for gangue filling materials: (a) vertical dumping system of gangue; (b) gangue conveyor.

The acceleration values of gangues with different particle sizes were basically the same within 2 s of falling, so the velocity of gangues with different particle sizes is also basically the same [100]. After 2 s, their accelerations showed obvious differences. The smaller the particle size, the faster the acceleration reached zero, and the faster it became a uniform motion. The larger the particle size, the longer the acceleration process and the faster the final velocity. This reflects that the influence of the air resistance on the gangue with a small particle size was significantly greater than that of the gangue with a large particle size, as shown in Figure 27a.

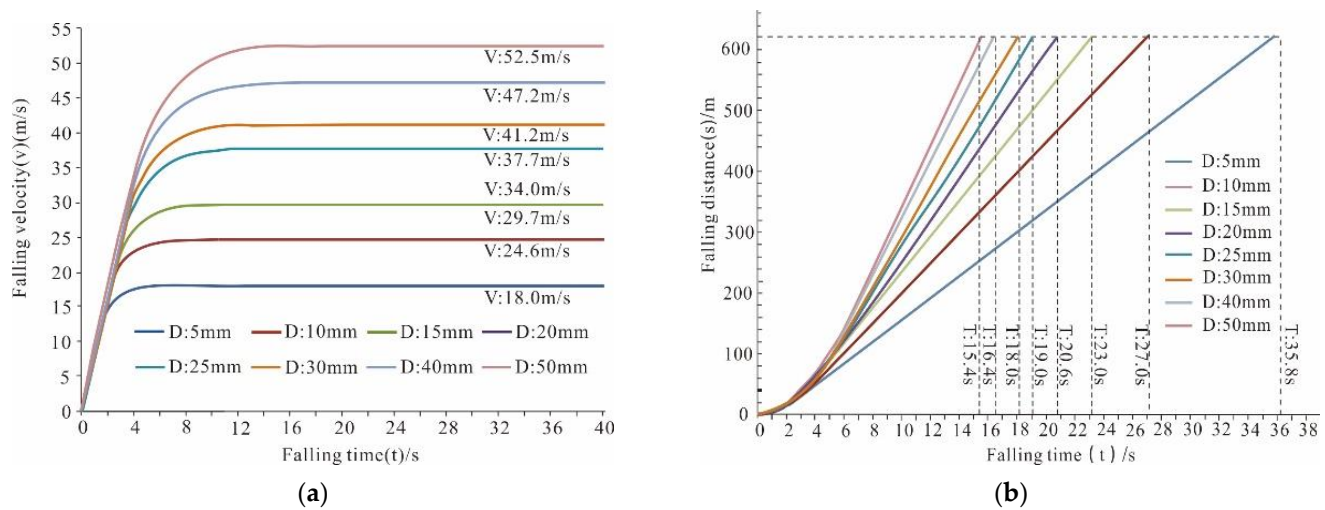


Figure 27. (a) The relationship between grain sizes of gangue; (b) running speed and time in the vertical pipeline.

The running time of the gangue in the vertical pipeline is negatively correlated with the grain size of the gangue; that is, the larger the grain size of the gangue, the shorter the running time of the gangue in the vertical pipeline. For example, when the grain size of the gangue increased from 5 mm to 50 mm, the running time of the gangue in a vertical pipeline as long as 620 m decreased from 35.8 s to 15.4 s, as shown in Figure 27b.

3.1.3. Activation of the Gangue Backfilling Material

Gangue is a granular material, and its deformation under load mainly comes from two aspects: on the one hand, the deformation of gangue particles themselves and, on the other hand, the closure of gaps between gangue particles. The latter usually accounts for a larger proportion than the former. Therefore, the compactness of the gangue filling materials is the most important factor affecting its bearing performance [101,102]. The compactness of the gangue filling material (D) is mainly regulated in the following two ways.

Controlling the grain gradation of gangue filling materials: In 2010, Wang et al. studied the influence of the gangue particle size on its bearing capacity through a consolidation experiment. It was found that gangue particles with a large particle size were easily crushed at the edges and corners, and the small particles generated would fill the gaps between the large particles, leading to gangue filling materials with a large particle size being more likely to produce compression deformation under the pressure of the overlying strata, and its supporting effect on the overlying strata in the goaf was weaker than that of gangue filling materials with a small grain size [92,94,103]. In 2012, Li et al. further studied the influence of the gangue particle size class on its bearing performance through a consolidation experiment. It was found that when the gangue filling materials configured with Talbol grading theory were compacted to a certain extent, the large gangue particles formed a skeleton structure, reducing the probability of particle rearrangement, and the gangue particles with a small particle size filled the pores between the large particles. The result was that the small particles were in close contact with the large particles, which increased the coordination number of the large particles and reduced the breakage of the large particles, and the skeleton force chain remained in a stable structural state. At this time, the anti-deformation ability of gangue filling materials was enhanced, and the control effect on the stability of the overlying strata in the goaf improved [64,92,104]. In 2015, Ou et al. applied foundation theory to study the influence law of the gangue particle size class on its bearing performance. It was found that the foundation coefficient of the gangue filling material with continuous gradation was larger than that of discontinuous gradation, as shown in Figures 28 and 29. Under the same pressure strength, the gangue filling body with continuous gradation was more difficult to compress. In order to ensure the filling

effect and make the mechanical properties of the gangue filling body more reliable, the foundation coefficient of the gangue filling body should be greater than 0.15 GPa/m [105].

$$P = 100 \left(\frac{d}{D} \right)^n \quad (32)$$

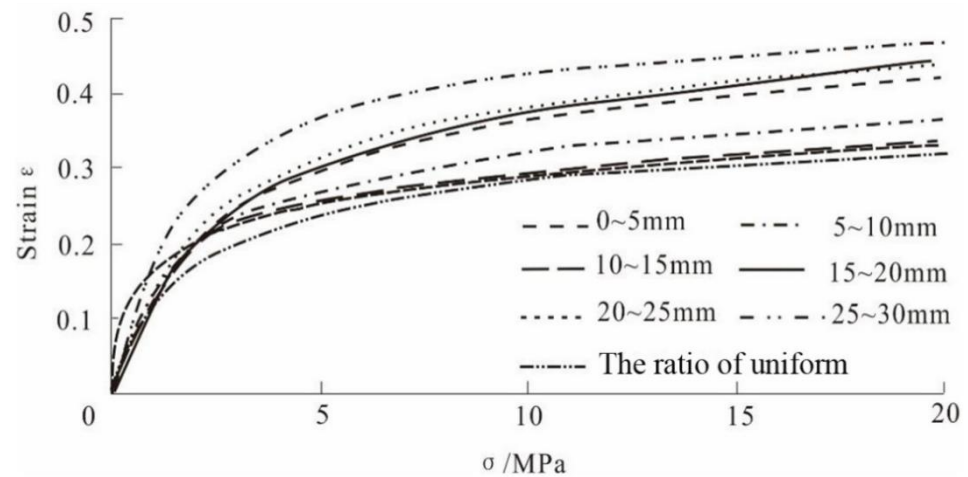


Figure 28. Consolidation curves of gangue with different grain gradations [94].

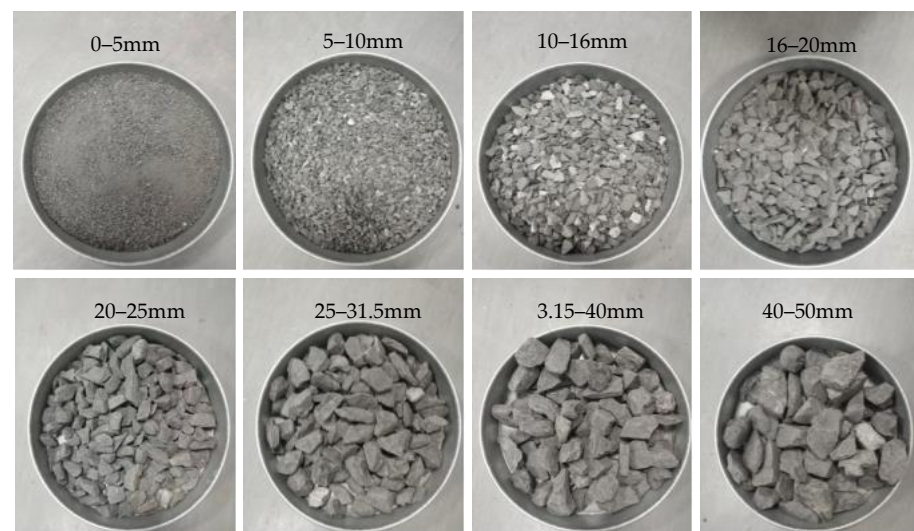


Figure 29. Photos of gangue with different grain sizes [106].

Here, P is the percentage of the gangue with each grain size, %; D is the maximum grain size of the gangue, mm; d is the current grain size of the gangue, mm; n is the Talbot index, and the value of n ranges from 0.3 to 0.7.

Controlling the tamping technology of gangue filling materials: In 2010, Wang et al. studied the influence law of the tamping angle and tamping speed on the compactness of gangue filling materials in the gob using EDEM discrete element numerical simulation software. It was found that with the increase in the tamping angle, the compactness of the gangue filling material in the gob increased first and then decreased. When the tamping angle was 27° , the compactness of the gangue filling material was at the maximum. With the increase in the tamping speed, the compactness of the gangue filling material showed a trend of a linear increase. This is because different tamping speeds exert different kinetic energy on gangue. The higher the tamping speed, the greater the kinetic energy of bulk materials and the greater the possibility of gangue particles flying away, which is less conducive to the compaction of gangue filling materials [98].

3.1.4. Time Needed to Fill the Post-Mining Space with Gangue Backfill Material

Compared with the previous several filling materials, gangue filling materials do not need water in the use process, so the goaf filling with gangue filling materials is not affected by water either. Due to the loss of water lubrication, the transportation and filling time of gangue backfilling materials are mainly determined by the corresponding mechanical efficiency. In particular, after gangue material is filled into the goaf, it needs to be precompacted, which is a time-consuming process. At present, the gangue filling capacity can reach 200 tons per hour, which can meet the filling demand of 1.2 million tons for a coal mine annually [100].

3.1.5. Evaluation of Gangue Backfilling Material

Advantages: Firstly, there is no need to consume water in the transportation and activation stages of the gangue backfilling material compared with the previous three backfilling materials. The gangue backfilling material method not only preserves water resources but also simplifies backfilling operations. Last but not least, gangue backfilling can effectively eliminate the impact of gangue on the mining environment. On the one hand, the coal in gangue will spontaneously combust after contact with air, releasing carbon dioxide and hydrogen sulfide gas, contributing to the greenhouse effect and acid rain. On the other hand, the heavy metal elements in gangue will migrate to the nearby soil and water under long-term weathering and rain leaching, resulting in soil and water pollution. The above problems can be solved by filling gangue into the goaf as raw material [107–109].

Disadvantages: First, the use cost of gangue filling materials is high. Although the cost of gangue materials is low, the gangue filling materials need special mechanical equipment in the process of crushing, horizontal transportation, and goaf filling, and they will consume a lot of energy, which reduces the overall technical feasibility of the gangue filling system. For example, a gangue filling system with an annual filling energy of 1 million tons needs an initial investment of USD 8 million. Secondly, the sources of gangue filling materials are insufficient. According to statistics, gangue accounts for approximately 30% of coal production in China's coal mining industry. Theoretically, the amount of gangue is only enough to fill approximately 30% of the goaf space. With the increase in the number of roadways in the coal seam and the decrease in the number of roadways in the rock stratum, the yield of gangue is gradually decreasing. Especially in some newly built mines, the quantity of gangue is far less than the requirement for dense filling in the goaf [110].

4. Expectation of Backfilling Material Selection in China

At present, the mining depth of China's coal mines generally ranges from 500 to 1000 m, and the filling work is also completed within this depth [111,112]. In addition, relevant investigations and studies show that coal resources buried more than 1000 m deep account for 53% of the total proven coal resources, with an average mining depth of 1086 m. As of December 2020, there were still 132 pairs of mine shafts in production due to the fact of an earthquake disaster in China, accounting for more than 10% of the total production capacity of the country's coal mines. The coal mining depth is also extended at a rate of 8–25 m per year, and the deep mining of long-developed mines in Central and East China tends to be normal [113,114].

Through the review and introduction of the above four filling and retrieval methods, we can roughly understand their advantages and disadvantages, as shown in Figure 30. **Hydraulic backfill:** The hydraulic backfill material is always composed of water and solid aggregate. Aggregate is mixed with water before transportation and floats in the slurry due to the buoyancy of the water. It has the advantage that the requirements for the backfill materials are easy to meet and the skill requirements for backfill operations are relatively low. **Cemented backfill:** The cemented backfill materials used commonly consist of water, cementing agents and coarse and fine aggregates. The coarse and fine aggregates are transported to the extraction area under the buoyancy of the slurry. The advantage is that the backfill material can be transported more efficiently and with greater mechanical

strength. High-water backfill: High-water backfill materials are mainly divided into two parts, where one part consists of material A and its auxiliary material AA, and the other part consists of material B and its auxiliary material BB. The high-water level fill is pumped to the mined-out area by Slurry A and Slurry B. This has the advantages of further improved transport efficiency and strong adaptability to different filling conditions. Gangue backfill: Gangue is usually broken into seven particle size groups: ≤ 5 mm, 5~10 mm, 10~20 mm, 20~30 mm, 30~40 mm, 40~50 mm, and ≥ 50 mm. Gangue filling materials can rely on their own gravity as the power for vertical movement, while horizontal transportation requires additional mechanical assistance. This has the advantages of saving water resources, simplifying backfilling operations and effectively eliminating the impact of gangue on the mining environment.

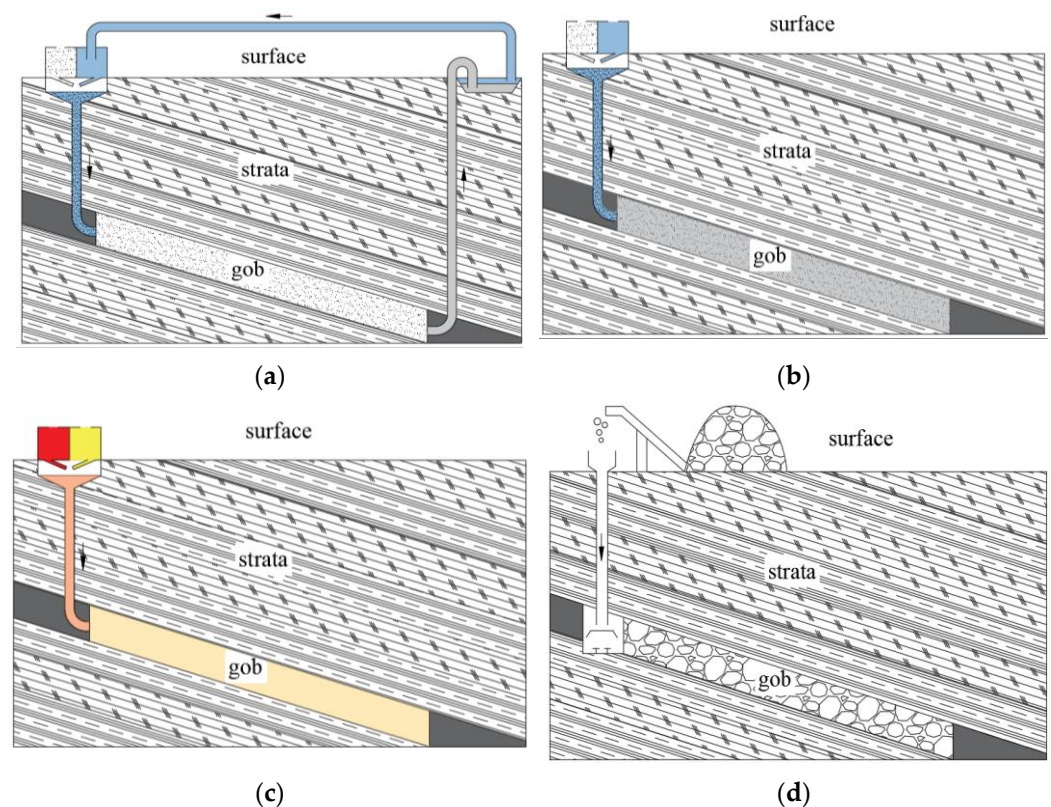


Figure 30. Transportation routes of backfilling materials under different filling methods: (a) hydraulic backfill; (b) cemented backfill; (c) high-water backfill; (d) gangue backfill.

China's coal mining center is gradually shifting from the central and eastern regions to the northwest region. In recent years, with the continuous promotion of China's "Belt and Road" strategy, the development of northwest China is gradually increasing. There are a large amount of coal resources in the northwest of China. For example, the coal reserves of Xinjiang and Inner Mongolia account for 40% and 21% of the total coal reserves of China [115]. The exploitation and utilization of these resources can provide powerful material and energy guarantees for China's rapid development. Unfortunately, years of large-scale coal mining have led to the depletion of easily accessible coal resources in Central and East China. It is difficult to exploit the remaining coal resources in the Midwest. For example, when mining the coal resources at deeper depths, the challenges of dynamic disasters, including rock bursts and coal and gas outbursts caused by high ground stress, are likely to be encountered. When mining coal resources under buildings, water bodies and railways, where small surface subsidence is required, filling mining should be adopted to control the overburden movement caused by coal mining within an acceptable range [116,117]. As a result of the above two reasons, China's coal mining center

is gradually shifting from the central and eastern regions to the northwest region, as shown in Figure 31.

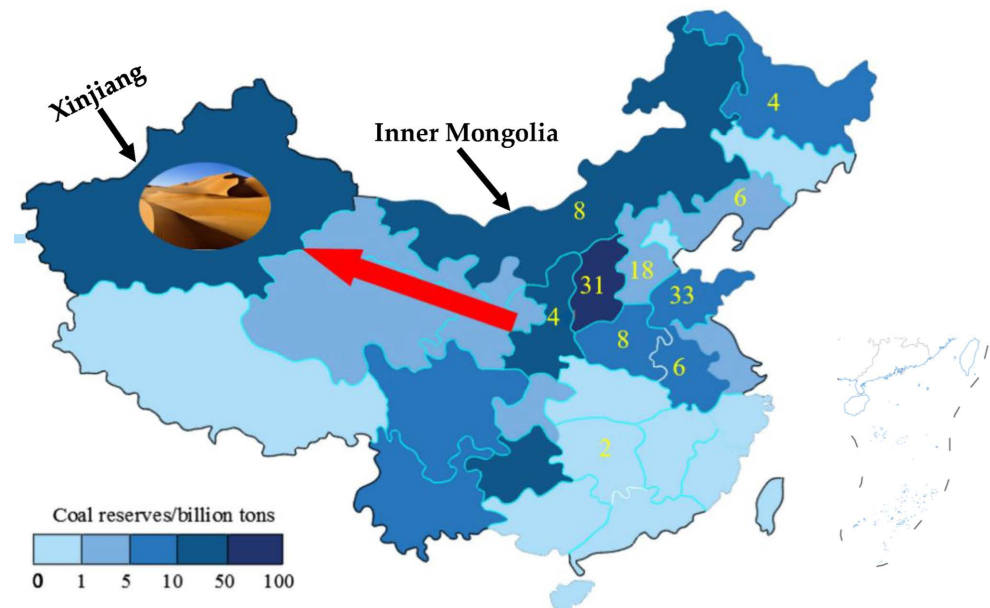


Figure 31. Distribution of coal resources and backfill mining projects in China. The numbers represent the amount of coal reserves in tons.

Serious ecological problems will be encountered when the traditional caving method is used to exploit coal resources in Northwest China. Firstly, the coal resources in the mining areas of Western China are generally shallow, thick and thin. Mining by the traditional caving method easily causes severe overburden movement, resulting in the loss of groundwater resources and surface collapse. Second, there is a long distance between the east and the west of China, and the transportation cost of raw coal is high [6,118]. As a result, the coal mined in the west of China can only be transformed locally and supports the construction of the economically developed areas along the southeast coast by the way of long-distance high-voltage electric energy transmission. Large-scale coal thermal power generation is bound to produce a large amount of fly ash and carbon dioxide, which will not only occupy land and pollute the environment but also aggravate the regional greenhouse effect and accelerate the evaporation of surface water resources. Consequently, drought and desertification will be further aggravated. This seriously affects the coordinated healthy development of the social, economic and ecological environment in the region, as shown in Figure 32.

Aeolian sand backfill mining is an effective way to realize the green mining of coal resources in northwest China. In order to comprehensively consider geological disasters and environmental damage in the process of coal development and utilization, a novel model that can realize green mining and low carbon utilization synchronously of the coal resources in the large coal power base in northwest China was proposed, as shown in Figure 33a. Firstly, the stability of the overlying rock in the goaf can be maintained by strip filling and then carbon dioxide gas generated by thermal power plants can be injected into the interval of the strip filling. The coal resources in Northwest China are mainly distributed in large sedimentary basins, such as the Tarim Basin and Junggar Basin [119]. The abundant aeolian sand on the surface of these areas is the ideal backfill material for the underground goaf. However, natural aeolian sand is a kind of granular material with poor particle size gradation (Figure 33b). It is necessary to improve the mechanical strength of natural aeolian sand in the following two ways to make it a qualified goaf backfill material.

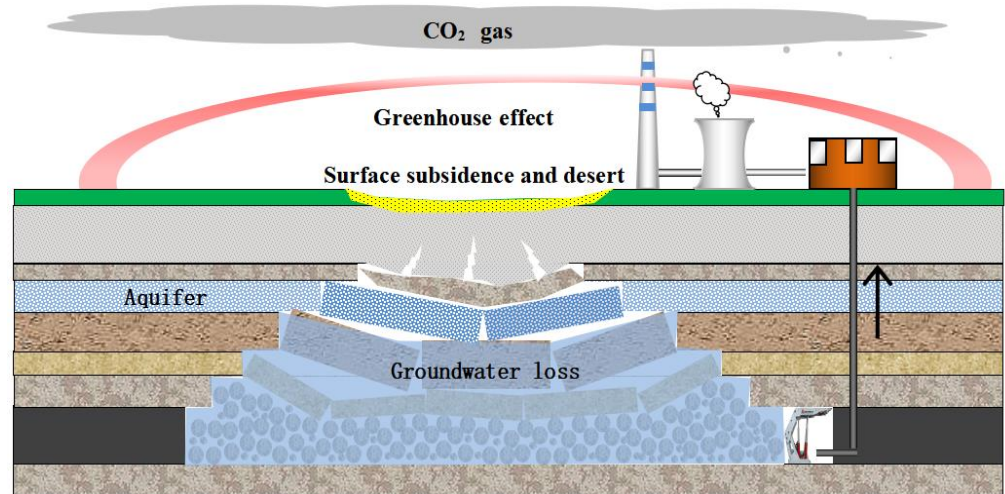


Figure 32. Ecological environmental problems of the large coal power base in Northwest China.

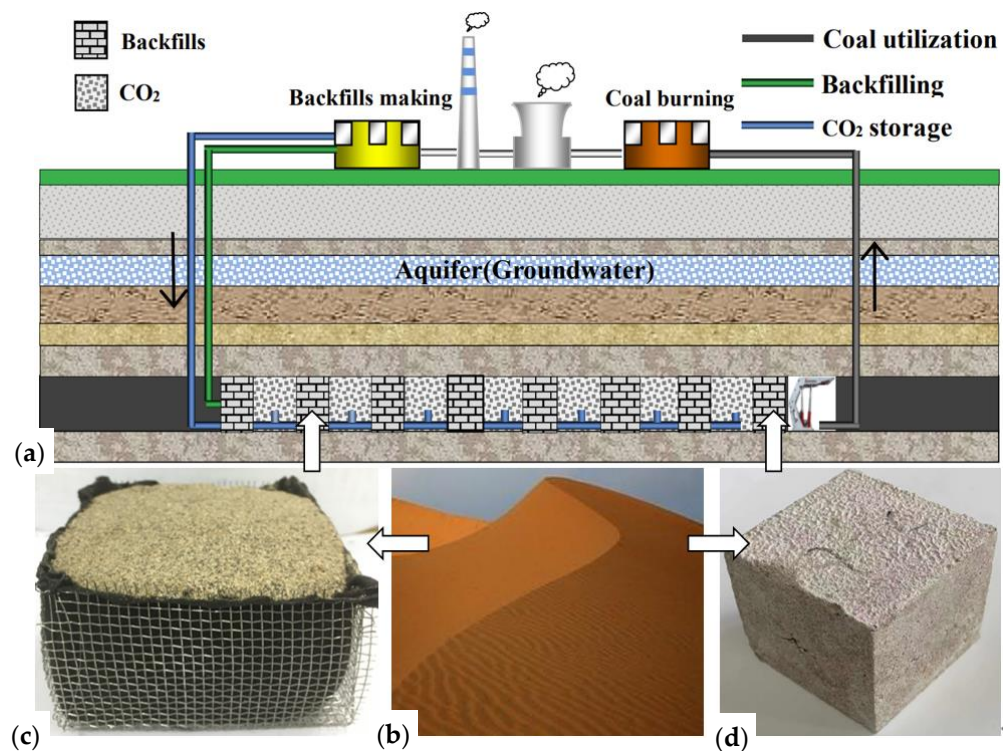


Figure 33. (a) A novel green mining model; (b) natural aeolian sand; (c) aeolian sand with lateral constraints; (d) aeolian sand with cementing agents.

Providing lateral constraints for aeolian sand: It can be known from the previous analysis of gangue backfill materials that aeolian sand particles are not only small in size but also high in strength, which makes the volume of aeolian sand difficult to compress. The above characteristics of aeolian sand mean that as long as aeolian sand is provided with certain lateral constraints, aeolian sand will have a corresponding longitudinal bearing capacity, and the greater the lateral constraints, the stronger the longitudinal bearing capacity [120]. Considering the technical economy of backfilling mining, a closed structure composed of a metal cage and geotextile may be an ideal choice, as shown in Figure 33c.

Providing cementation for aeolian sand: According to the analysis of cemented backfill materials, the cohesion of aeolian sand can be effectively improved by cementing the scattered aeolian sand particles together by the action of a cementing agent [121]. After that, aeolian sand could become a qualified gob backfill material with bearing capacity.

Considering the technical economy of backfilling mining, the fly ash produced by coal-fired power plants near coal mines may be an ideal choice, as shown in Figure 33d.

5. Conclusions

In this paper, the primary considerations of the main backfill materials employed successfully in Chinese underground coal mining were analyzed during the preparation, transportation and activation stages, followed by an evaluation of each backfill material. Based on the above analysis, suggestions for backfill material exploration were proposed in terms of the oncoming backfill mining of the coal deposit located in Northwest China with serious sandy desertification. The main conclusions are as follows.

According to statistics on backfill mining practices in major coal-mining provinces in China, the main backfill materials employed successfully in underground coal mines can be divided into two categories—water-involving backfill materials and waterless backfill materials—depending on whether water is used during the backfill mining operations. Furthermore, the former involves hydraulic backfill materials, accounting for 10%, cemented backfill materials, accounting for 30%, and high-water backfill materials, accounting for 20%. The latter covers gangue backfill materials, accounting for 20%, and other solid waste that is occasionally used.

The most significant feature of the water-involving backfill materials is that water is used as the transportation medium of the solid filling aggregates. In order to eliminate the hydraulic backfill materials' segregation problem during long-distance transportation, cemented backfill materials are proposed by increasing the filling slurry's concentration by adding cementing agents and fine aggregates, while high-water backfill materials look in the opposite direction for a solution, that is, by reducing the filling slurry's concentration via adding a small amount of chemicals and a large amount of water. Consequently, not only the transportation performance of the modified filling material is improved impressively, but also its bearing strength is greatly enhanced.

The most significant advantages of waterless backfill materials are that the water consumption can be completely eliminated during backfill operations and solid waste on the ground can be backfilled underground. Gangue aggregates can slide underground via the force of gravity and can be further transported horizontally into the gob through additional mechanical assistance. An appropriate grading and compactness are required for a desired backfill effect. Unfortunately, a large amount of investment in equipment and the destined shortage in quantity become the biggest obstacles to the wide application of this method.

China's coal mining center is gradually shifting from the central and eastern regions to the northwest region. Serious ecological problems will be encountered when the traditional caving method is used to exploit the coal resources there. Aeolian sand will be a perfect choice of filling material in the northwest mining area, which has serious drought and desertification. Considering the technique—the economics of backfill mining, lateral constraints and cohesion could be imposed on dispersive aeolian sand for a desired bearing strength through a metal cage and fly ash, and the specific cage strength and fly ash properties need to be studied in the future.

6. Patents

(1) Zhang, Z.Y.; Guan, W.M.; Lv, J.X. A method of constructing the wall of retaining roadway along gob by net box with aeolian sand inside, China National Invention patent, ZL2018112400713, Authorization Announcement date 16 October 2020.

(2) Zhang, Z.Y.; Zhang, J.H.; Chen, H. A method of backfilling the underground gob by net box with aeolian sand inside, China National Invention patent, ZL2018112400840, Authorization Announcement date 16 October 2020.

(3) Zhang, Z.Y.; Lv, J.X.; Chen, H. A continuous mining method of rigid and flexible strip filling without coal pillar in goaf in inclined coal seam, China National Invention patent, ZL2018114711562, Authorization Announcement date 2 February 2021.

Author Contributions: Conceptualization, Z.Z. and J.F.; methodology, W.W. and J.F.; validation, X.X. and W.G.; formal analysis, H.L. and J.F.; investigation, W.G. and J.F.; data curation, H.S. and B.Z.; writing—original draft preparation, D.H. and Y.S.; writing—review and editing, Z.Z.; funding acquisition, Z.Z. All authors have read and agreed to the published version of the manuscript.

Funding: This research was funded by the National Natural Science Foundation of China (51964042).

Data Availability Statement: Not applicable.

Acknowledgments: We acknowledge the library staff of Xinjiang University for their help in literature retrieval. We are also grateful to the editors and reviewers for their comments on this paper.

Conflicts of Interest: The authors declare no conflict of interest.

References

1. Qi, H.Y. Analysis on production status and safety situation for developed country of coal industry. *China Coal* **2015**, *41*, 140–143.
2. Zhang, Z.Y.; Shimada, H.; Sasaoka, T.; Hamanaka, A. Stability Control of Retained Goaf-Side Gateroad under Different Roof Conditions in Deep Underground Y Type Longwall Mining. *Sustainability* **2017**, *9*, 1671. [[CrossRef](#)]
3. Liu, X.; Jing, M.; Bai, Z. Heavy Metal Concentrations of Soil, Rock, and Coal Gangue in the Geological Profile of a Large Open-Pit Coal Mine in China. *Sustainability* **2022**, *14*, 1020. [[CrossRef](#)]
4. Hao, Y.; Xie, T. Oxidation Behavior and Kinetics Parameters of a Lean Coal at Low Temperature Based on Different Oxygen Concentrations. *Minerals* **2021**, *11*, 511. [[CrossRef](#)]
5. Qu, Q.; Guo, H.; Yuan, L.; Shen, B.; Yu, G.; Qin, J. Rock Mass and Pore Fluid Response in Deep Mining: A Field Monitoring Study at Inclined Longwalls. *Minerals* **2022**, *12*, 463. [[CrossRef](#)]
6. Qian, M.G.; Xu, J.L.; Miao, X.X. Green Technique in Coal Mining. *J. China Univ. Min. Technol.* **2003**, *04*, 5–10.
7. Rajwa, S.; Janoszek, T.; Świątek, J.; Walentek, A.; Bałaga, D. Numerical Simulation of the Impact of Unmined Longwall Panel on the Working Stability of a Longwall Using UDEC 2D—A Case Study. *Energies* **2022**, *15*, 1803. [[CrossRef](#)]
8. Zhang, Z.Y.; Liu, H.; Su, H.; Zeng, Q. Green Mining Takes Place at the Power Plant. *Minerals* **2022**, *12*, 839. [[CrossRef](#)]
9. Xie, S.; Guo, F.; Wu, Y. Control Techniques for Gob-Side Entry Driving in an Extra-Thick Coal Seam with the Influence of Upper Residual Coal Pillar: A Case Study. *Energies* **2022**, *15*, 3620. [[CrossRef](#)]
10. Wang, X.; Zhang, J.; Li, M.; Gao, F.; Taheri, A.; Huo, B.; Jin, L. Expansion Properties of Cemented Foam Backfill Utilizing Coal Gangue and Fly Ash. *Minerals* **2022**, *12*, 763. [[CrossRef](#)]
11. Korzeniowski, W.; Poborska Mlynarska, K.; Skrzypkowski, K. The idea of the recovery of Municipal Solid Waste Incineration (MSWI) residues in Klodawa salt mine S.A. by filling the excavations with self-solidifying mixtures. *Arch. Min. Sci.* **2018**, *63*, 3.
12. Skrzypkowski, K. Compressibility of materials and backfilling mixtures with addition of solid wastes from flue-gas treatment and fly ashes. *E3S Web Conf.* **2018**, *71*, 7. [[CrossRef](#)]
13. Ajayi, S.A.; Ma, L.; Spearing, A.J.S. Ground Stress Analysis and Automation of Workface in Continuous Mining Continuous Backfill Operation. *Minerals* **2022**, *12*, 754. [[CrossRef](#)]
14. Cao, H.; Gao, Q.; Zhang, X.; Guo, B. Research Progress and Development Direction of Filling Cementing Materials for Filling Mining in Iron Mines of China. *Gels* **2022**, *8*, 192. [[CrossRef](#)]
15. Wu, C.; Zhang, Y.; Zhang, J.; Chen, Y.; Duan, C.; Qi, J.; Cheng, Z.; Pan, Z. Comprehensive Evaluation of the Eco-Geological Environment in the Concentrated Mining Area of Mineral Resources. *Sustainability* **2022**, *14*, 6808. [[CrossRef](#)]
16. Liu, J.; Ma, F.; Guo, J.; Li, G.; Song, Y.; Wang, Y. A Field Study on the Law of Spatiotemporal Development of Rock Movement of Under-Sea Mining, Shandong, China. *Sustainability* **2022**, *14*, 5864. [[CrossRef](#)]
17. Adach-Pawelus, K.; Pawelus, D. Application of Hydraulic Backfill for Rockburst Prevention in the Mining Field with Remnant in the Polish Underground Copper Mines. *Energies* **2021**, *14*, 3869. [[CrossRef](#)]
18. Li, L.; Huang, Q.; Zuo, X.; Wu, J.; Wei, B.; He, Y.; Zhang, W.; Zhang, J. Study on the Slurry Diffusion Law of Fluidized Filling Gangue in the Caving Goaf of Thick Coal Seam Fully Mechanized Caving Mining. *Energies* **2022**, *15*, 8164. [[CrossRef](#)]
19. Xu, G.G.; Wang, X.D.; Wang, H.; Shao, H.Q.; Cao, Z.B. Treatment technology of cavitory gob area based on high concentration cemented filling material. *Coal Eng.* **2021**, *53*, 73–80.
20. Skrzypkowski, K. Determination of the Backfilling Time for the Zinc and Lead Ore Deposits with Application of the BackfillCAD Model. *Energies* **2021**, *14*, 3186. [[CrossRef](#)]
21. Xu, W.B.; Du, J.H.; Song, W.D.; Chen, H.Y. Experiment on the mechanism of consolidating backfill body of extra-fine grain unclassified tailings and cementitious materials. *Rock Soil Mech.* **2013**, *34*, 2295–2302.
22. Jia, Z.G. Experimental study on failure characteristics of strata with different filling rates in longwall filling mining. *Coal Sci. Technol.* **2019**, *47*, 197–202.
23. Wei, X.M.; Guo, S.J.; Li, Z.N. Study on the strength difference of cemented backfill based on macro-micro coupling analysis. *China Min. Mag.* **2018**, *27*, 95–99.
24. Yu, W.J.; Wan, X.; Liu, F.F.; Wang, Z. Experimental study on red clay paste backfilling material and its physical characteristics. *Coal Sci. Technol.* **2021**, *49*, 61–68.

25. Li, M.H.; Yang, Z.Q.; Wang, Y.T.; Gao, Q. Experiment study of compressive strength and mechanical property of filling body for fly ash composite cementitious materials. *J. China Univ. Min. Technol.* **2015**, *44*, 650–655.
26. Feng, G.M.; Ding, Y.; Zhu, H.J. Bai Jianbiao Experimental study on mining ultra-high water filling material and its structure. *J. China Univ. Min. Technol.* **2010**, *39*, 813–819.
27. Zhou, G.M.; Ma, Y.D.; Li, X.T. Study on compression deformation characteristics of high solid water filling materials with different water content. *J. Jiangsu Constr. Vocat. Tech. Coll.* **2019**, *19*, 1–6.
28. Amin, M.N.; Iqbal, M.; Ashfaq, M.; Salami, B.A.; Khan, K.; Faraz, M.I.; Alabdullah, A.A.; Jalal, F.E. Prediction of Strength and CBR Characteristics of Chemically Stabilized Coal Gangue: ANN and Random Forest Tree Approach. *Materials* **2022**, *15*, 4330. [[CrossRef](#)]
29. Zhao, Y.S.; Du, X.L.; Dang, P.; Liu, G.J. Design on High-Concentration Cemented Filling Station in Xinyang Coal Mine. *Coal Eng.* **2014**, *46*, 31–33.
30. Wen, P.; Guo, W.; Tan, Y.; Bai, E.; Ma, Z.; Wu, D.; Yang, W. Paste Backfilling Longwall Mining Technology for Thick Coal Seam Extraction under Buildings and above Confined Aquifers: A Case Study. *Minerals* **2022**, *12*, 470. [[CrossRef](#)]
31. Wang, X.M.; Ding, D.Q.; Wu, Y.B.; Zhang, Q.L.; Lu, Y.Z. Numerical simulation and analysis of paste backfilling with piping transport. *China Min. Mag.* **2006**, *07*, 57–59+66.
32. Zhao, C.Z.; Zhou, H.Q.; Bai, J.B.; Qiang, H. Influence factor analysis of paste filling material strength. *J. Liaoning Tech. Univ.* **2006**, *25*, 904–906.
33. Zhao, C.Z.; Zhou, H.Q.; Qu, Q.D.; Chang, Q.L. Experimental study on rheology performances of paste backfilling slurry. *Coal Sci. Technol.* **2006**, *34*, 54–56.
34. Luan, H.; Jiang, Y.; Lin, H.; Wang, Y. A New Thin Seam Backfill Mining Technology and Its Application. *Energies* **2017**, *10*, 2023. [[CrossRef](#)]
35. Cheng, Q.; Guo, Y.; Dong, C.; Xu, J.; Lai, W.; Du, B. Mechanical Properties of Clay Based Cemented Paste Backfill for Coal Recovery from Deep Mines. *Energies* **2021**, *14*, 5764. [[CrossRef](#)]
36. Lv, W.; Guo, K.; Wang, H.; Feng, K.; Jia, D. Evolution Characteristics of Overlying Strata Fractures in Paste Composite Filling Stope. *Minerals* **2022**, *12*, 654. [[CrossRef](#)]
37. Yin, B.; Kang, T.; Kang, J.; Chen, Y. Experimental and Mechanistic Research on Enhancing the Strength and Deformation Characteristics of Fly-Ash-Cemented Filling Materials Modified by Electrochemical Treatment. *Energy Fuels* **2018**, *32*, 3614–3626. [[CrossRef](#)]
38. Xu, Y.; Ma, L.; NGO, I.; Zhai, J. Continuous Extraction and Continuous Backfill Mining Method Using Carbon Dioxide Mineralized Filling Body to Preserve Shallow Water in Northwest China. *Energies* **2022**, *15*, 3614. [[CrossRef](#)]
39. Zhang, W.; Yan, C.; Zhou, G.; Guo, J.; Chen, Y.; Zhang, B.; Wu, S. Experimental and Analytical Investigation into the Synergistic Mechanism and Failure Characteristics of the Backfill-Red Sandstone Combination. *Minerals* **2022**, *12*, 202. [[CrossRef](#)]
40. Rong, K.; Lan, W.; Li, H. Industrial Experiment of Goaf Filling Using the Filling Materials Based on Hemihydrate Phosphogypsum. *Minerals* **2020**, *10*, 324. [[CrossRef](#)]
41. Wu, J.; Feng, M.; Xu, J.; Qiu, P.; Wang, Y.; Han, G. Particle Size Distribution of Cemented Rockfill Effects on Strata Stability in Filling Mining. *Minerals* **2018**, *8*, 407. [[CrossRef](#)]
42. Yu, L.; Xia, J.; Gu, J.; Zhang, S.; Zhou, Y. Degradation Mechanism of Coal Gangue Concrete Suffering from Sulfate Attack in the Mine Environment. *Materials* **2023**, *16*, 1234. [[CrossRef](#)]
43. Leng, Q.; Chang, Q.; Sun, Y.; Zhang, B.; Qin, J. The Mechanical Properties of Gangue Paste Material for Deep Mines: An Experimental and Model Study. *Materials* **2022**, *15*, 5904. [[CrossRef](#)]
44. Liu, X.H.; Cui, S.L.; Zhao, J.L.; Tian, L.T.; Chen, L.; Zhao, T.Y. Top coal caving longwall mining in high coal seams under Yuecheng Reservoir: An engineering practice. *China Coal* **2009**, *35*, 66–67+87.
45. Zhao, C.Z.; Zhou, H.Q.; Bai, J.B.; Chang, Q.L. Experimental Research on Fly Ash Total Tailing Paste Filling. *Met. Mine* **2006**, *12*, 4–6.
46. Wang, X.; Zhang, J.; Li, M.; Huo, B.; Jin, L. Experimental Study on Performance Optimization of Grouting Backfill Material Based on Mechanically Ground Coal Gangue Utilizing Urea and Quicklime. *Materials* **2023**, *16*, 1097. [[CrossRef](#)] [[PubMed](#)]
47. Guo, Z.H.; Zhou, H.Q.; Wu, L.F.; Li, F. Numerical Simulation for Roof and Surface Subsidence Process Caused by Paste Filling. *J. Min. Saf. Eng.* **2008**, *25*, 172–175.
48. Sun, Q.; Zhang, X.D.; Yang, Y. Creep constitutive model of cemented body used in backfilling mining. *J. China Coal Soc.* **2013**, *38*, 994–1000.
49. Yang, Z.; Wang, Q.Y.; Wang, N.; Cao, Q.H.; Ma, C.Y. Research on the “eggshell” phenomenon of the backfilling materials with cement fly ash and waste rocks. *J. Qingdao Technol. Univ.* **2012**, *33*, 49–53.
50. Zheng, S.C.; Yu, Q.; Ning, P.; Ma, J.B.; Tian, L.; Zheng, Y.L. Effects and mechanism of anhydrite AIII on the performance of β -hemihydrate gypsum. *J. Civ. Archit. Environ. Eng.* **2015**, *37*, 118–124.
51. Liu, Y.; Chen, J. Research status and development trend of high sand filling materials. *Key Eng. Mater.* **2017**, *727*, 1079–1083. [[CrossRef](#)]
52. Li, J.S. Influence of early strength agent on strength development of cemented backfill material. *Non Ferr. Metals* **2000**, *5*, 18–19.
53. Zhou, N.; Ma, H.; Ouyang, S.; Germain, D.; Hou, T. Influential Factors in Transportation and Mechanical Properties of Aeolian Sand-Based Cemented Filling Material. *Minerals* **2019**, *9*, 116. [[CrossRef](#)]
54. Shao, X.; Tian, C.; Li, C.; Fang, Z.; Zhao, B.; Xu, B.; Ning, J.; Li, L.; Tang, R. The Experimental Investigation on Mechanics and Damage Characteristics of the Aeolian Sand Paste-like Backfill Materials Based on Acoustic Emission. *Materials* **2022**, *15*, 7235. [[CrossRef](#)]
55. Wang, L.; Wang, C.L.; Sun, D.S.; Zhang, G.Z.; Wang, A.G. Experimental research on rheology characteristics of roadside support backfilling concrete. *J. Anhui Inst. Archit. Ind.* **2010**, *18*, 76–80.

56. Zhang, X.; Lin, J.; Liu, J.; Li, F.; Pang, Z. Investigation of Hydraulic-Mechanical Properties of Paste Backfill Containing Coal Gangue-Fly Ash and Its Application in an Underground Coal Mine. *Energies* **2017**, *10*, 1309. [[CrossRef](#)]
57. Wang, H.; Zhao, X.; Zhou, B.; Lin, Y.; Gao, H. Performance Optimization and Characterization of Soda Residue-Fly Ash Geopolymer Paste for Goaf Backfill: Beta-Hemihydrate Gypsum Alternative to Sodium Silicate. *Materials* **2020**, *13*, 5604. [[CrossRef](#)]
58. Li, H.Y. *Study on Time-Dependent Changes in the Flow Properties of Cemented Coal Gangue Backfill Materials*; Taiyuan University of Technology: Taiyuan, China, 2019.
59. Li, F.; Yin, D.; Zhu, C.; Wang, F.; Jiang, N.; Zhang, Z. Effects of Kaolin Addition on Mechanical Properties for Cemented Coal Gangue-Fly Ash Backfill under Uniaxial Loading. *Energies* **2021**, *14*, 3693. [[CrossRef](#)]
60. Sun, Q.; Wei, X.; Li, T.; Zhang, L. Strengthening Behavior of Cemented Paste Backfill Using Alkali-Activated Slag Binders and Bottom Ash Based on the Response Surface Method. *Materials* **2020**, *13*, 855. [[CrossRef](#)]
61. Zheng, K.; Xuan, D.; Li, J. Study on Fluid–Solid Characteristics of Grouting Filling Similar-Simulation Materials. *Minerals* **2022**, *12*, 502. [[CrossRef](#)]
62. Yang, B.; Wang, X.; Yin, P.; Gu, C.; Yin, X.; Yang, F.; Li, T. The Rheological Properties and Strength Characteristics of Cemented Paste Backfill with Air-Entraining Agent. *Minerals* **2022**, *12*, 1457. [[CrossRef](#)]
63. Xiang, H.Q.; Yang, H.; Gong, Y.K.; Zhang, J. Phosphate Removal in Wastewater Treatment Using Property-modified Fly Ash. *Environ. Sci. Technol.* **2005**, *5*, 18–20.
64. Jia, L.T. Properties and Modification of Coal Fly Ash. *Power Gener. Air Cond.* **2017**, *38*, 35–38.
65. Qin, H.Y.; Ti, Z.Y.; Zhang, F.; Wang, H.D.; Ouyang, Z.H.; Li, X.B.; Peng, R. Determination of Equivalent Mining Height in Paste-like Filling Mining. *Coal Technol.* **2020**, *39*, 1–3.
66. Fu, X.L.; Peng, Y.H.; Li, D.; Cheng, K. Research on impact of water reducing agent for cemented tailing fill slurry conveying property. *Coal Sci. Technol.* **2017**, *45*, 55–60.
67. Yao, Z.Q.; Zhang, Q.L.; Wang, X.M. Application of water reducing agent in paste like cemented filling. *Saf. Coal Mines* **2009**, *40*, 43–45.
68. Liu, J. Application Status and Development of Filling Mining Method. *Mod. Chem. Res.* **2020**, *7*, 8–9.
69. Wang, X.M.; Lu, Y.Z.; Zhang, Q.L. Simulating and Optimizing the Configuration Parameter of Stope in Plaster -Like Filling. *Chin. J. Undergr. Space Eng.* **2008**, *4*, 346–350.
70. *Polish Standard PN-EN 196-3; Cement Test Methods-Part 3: Determination of Setting Times and Volume Stability*. Polish Committee for Standardization: Warsaw, Poland, 2006; p. 13.
71. Qi, C.; Guo, L.; Wu, Y.; Zhang, Q.; Chen, Q. Stability Evaluation of Layered Backfill Considering Filling Interval, Backfill Strength and Creep Behavior. *Minerals* **2022**, *12*, 271. [[CrossRef](#)]
72. Skrzypkowski, K. 3D Numerical Modelling of the Application of Cemented Paste Backfill on Displacements around Strip Excavations. *Energies* **2021**, *14*, 7750. [[CrossRef](#)]
73. Zuo, Y.F.; Wang, D.M.; Gao, Z.G.; Guo, Q.; Mei, S.G.; Liu, J.L. Effect of chemical structure and composition of polycarboxylate superplasticizer on cement hydration. *New Build. Mater.* **2016**, *43*, 25–29+42.
74. Zhao, Y. *Research on Red-Mud Based Cementitious Paste Goaf Backfill Materials and Its Environmental Performances*; Taiyuan University of Technology: Taiyuan, China, 2021. [[CrossRef](#)]
75. Zhang, J.; Li, M.; Taheri, A.; Zhang, W.; Wu, Z.; Song, W. Properties and Application of Backfill Materials in Coal Mines in China. *Minerals* **2019**, *9*, 53. [[CrossRef](#)]
76. Wang, X.; Qin, D.; Zhang, D.; Sun, C.; Zhang, C.; Xu, M.; Li, B. Mechanical Characteristics of Superhigh-Water Content Material Concretion and Its Application in Longwall Backfilling. *Energies* **2017**, *10*, 1592. [[CrossRef](#)]
77. Ding, Y.; Feng, G.M.; Wang, Z.C. Experimental study on basic properties of ultra-high water filling materials. *J. Coal* **2011**, *36*, 1087–1092.
78. Zhou, X.; Xu, H.B.; Liu, J.H. Study on instability failure characteristics and performance improvement of high water filling materials. *J. Coal* **2017**, *42*, 1123–1129.
79. Zhang, H.X.; Zhou, H.B.; Chen, F.Y.; Fen, T.; Sheng, S.H.; Wu, Z.G. research on Tianjin industry’s energy-short-age alleviation based on GFI model. *J. Saf. Environ.* **2015**, *15*, 295–299.
80. Peng, M.X.; Jiang, J.H.; Wang, Z.H.; Shen, S.H. Study on preparation, microstructure and curing mechanism of slurry solidified filling material. *Silic. Bull.* **2011**, *30*, 1294–1298.
81. Yu, L.M.; Wang, F.G.; Wang, J.; Lan, W.T. Study on fluidity of high water swelling material slurry. *Gansu Metall.* **2013**, *35*, 1–4+16.
82. Xie, S.R.; Zhang, G.C.; He, S.S.; Sun, Y.J. Surrounding rock control mechanism and application of gob retaining roadway in deep large mining height filling mining. *J. Coal* **2014**, *39*, 2362–2368.
83. Li, J.; Feng, G.M.; Jia, K.J.; Zhou, S.; Yao, F. Application Research on filling mining with ultra-high water material and retaining roadway along goaf. *Coal Eng.* **2013**, *45*, 10–12.
84. Hua, H.T. *Study on Roadway Side Filling and Gob Side Retaining Technology of New High Water Material in High Dip Thin Coal Seam*; China University of Mining and Technology: Beijing, China, 2015.
85. Bai, J.B.; Hou, C.J.; Zhang, C.G.; Yang, T.M.; Zhang, D.G.; Niu, H.W. Industrial test of filling empty roadway with high water content material. *Coal Sci. Technol.* **2000**, 30–31+39. [[CrossRef](#)]
86. Li, X.F.; Xiong, Z.Q.; Wang, X.; Sun, Y.P.; Jiang, T. Ultra high water material ratio and filling process optimization in filling mining of thin coal seam. *Coal Mine Saf.* **2020**, *51*, 162–167.

87. Gao, Y.G.; Ma, Q. Application Research of high water material gob side entry retaining technology in Yunjialing 12303 working face. *Coal Chem. Ind.* **2015**, *38*, 42–44+152.
88. Huang, P.; Spearing, S.; Ju, F.; Jessu, K.V.; Wang, Z.; Ning, P. Control Effects of Five Common Solid Waste Backfilling Materials on In Situ Strata of Gob. *Energies* **2019**, *12*, 154. [[CrossRef](#)]
89. Gu, W.; Chen, L.; Xu, D. Research on the Overburden Movement Law of Thick Coal Seam Without-Support Gangue-Filling Mining. *Minerals* **2023**, *13*, 53. [[CrossRef](#)]
90. Wang, S.; Lv, W.; Zhang, W.; Fan, J.; Luo, A.; Zhu, K.; Guo, K. Scale Effect of Filling on Overburden Migration in Local Filling Stope of Longwall Face in Steeply Dipping Coal Seam. *Minerals* **2022**, *12*, 319. [[CrossRef](#)]
91. Zhang, S.; Che, C.; Zhao, C.; Du, S.; Liu, Y.; Li, J.; Yang, S. Effect of Fly Ash and Steel Fiber Content on Workability and Mechanical Properties of Roadway Side Backfilling Materials in Deep Mine. *Energies* **2023**, *16*, 1505. [[CrossRef](#)]
92. Guo, G.L.; Miao, X.X.; Cha, J.F.; Ma, Z.G.; Zhou, Z.Y. Preliminary analysis on subsidence control effect of gangue filling mining in long wall face. *China Sci. Technol. Pap. Online* **2008**, *11*, 805–809.
93. Zhang, J.X.; Miao, X.X.; Guo, G.L. Development status of gangue (solid waste) direct filling coal mining technology. *J. Min. Saf. Eng.* **2009**, *26*, 395–401.
94. Ti, Z.Y.; Qin, H.Y.; Li, S.X. Experimental analysis on compaction characteristics of gangue filling. *J. Water Resour. Water Eng.* **2012**, *23*, 129–131.
95. Yang, Y.; Wang, B.F.; Zheng, Z.M. Experimental study on compaction energy consumption characteristics of coal mine gangue filling material. *Silic. Bull.* **2016**, *35*, 3511–3516.
96. Cui, J.K.; Zhang, H.; Li, Z.Y.; Luo, F.; Guo, L.J.; Wang, K. Comparative experimental study on compaction characteristics of gangue and fly ash. *Coal Technol.* **2017**, *36*, 284–287.
97. Geng, Q.Y.; Yao, S.Y.; Zhang, P.F.; Li, Z.H.; Liu, X.M. Analysis on Influencing Factors of overburden deformation monitoring and control effect in filling mining. *China Coal* **2018**, *44*, 46–49.
98. Han, X.L. *Study on Mechanical Response of Bulk Filling Material under Compaction*; China University of Mining and Technology: Beijing, China, 2017.
99. Li, M.; Zhang, J.X.; Miao, X.X.; Huang, Y.L. Study on the movement law of rock formation under the compaction characteristics of solid filling. *J. China Univ. Min. Technol.* **2014**, *43*, 969–973+980.
100. Li, J.; Huang, Y.; Chen, Z.; Li, M.; Qiao, M.; Kizil, M. Particle-Crushing Characteristics and Acoustic-Emission Patterns of Crushing Gangue Backfilling Material under Cyclic Loading. *Minerals* **2018**, *8*, 244. [[CrossRef](#)]
101. Qin, T.; Guo, X.; Huang, Y.; Wu, Z.; Qi, W.; Wang, H. Study on Macro-Meso Deformation Law and Acoustic Emission Characteristics of Granular Gangue under Different Loading Rates. *Minerals* **2022**, *12*, 1422. [[CrossRef](#)]
102. Yin, Y.; Zhao, T.; Zhang, Y.; Tan, Y.; Qiu, Y.; Taheri, A.; Jing, Y. An Innovative Method for Placement of Gangue Backfilling Material in Steep Underground Coal Mines. *Minerals* **2019**, *9*, 107. [[CrossRef](#)]
103. Li, X.W.; Zhao, X.Y.; Cheng, L.C.; Qin, Y.L. Experimental study on lateral compaction characteristics of gangue backfill under limited Roof. *Coal Sci. Technol.* **2020**, *48*, 18–24.
104. Xiao, M.; Ju, F.; He, Z.Q.; Li, K.Y.; Wang, P. Experimental study on Influencing Factors of side pressure coefficient of gangue filling material. *J. Min. Saf. Eng.* **2020**, *37*, 73–80.
105. Ou, Y. *Application of Gangue Filling Method in Upward Mining*; Hunan University of Science and Technology: Xiangtan, China, 2015.
106. MA, Y.D. *Study on the Macro-Micro Bearing Features of Different Polymer-Gangue Filling Material*; China University of Mining and Technology: Xuzhou, China, 2020. [[CrossRef](#)]
107. Liu, H.F.; Zhang, J.X.; Zhou, N.; Shen, L.L.; Zhang, L.B.; Zhu, C.L.; Wang, L. Study of the leaching and solidification mechanism of heavy metals from gangue-based cemented paste backfilling materials. *J. China Univ. Min. Technol.* **2021**, *50*, 523–531.
108. Guo, Y.X.; Zhao, Y.H.; Feng, G.R.; Ran, H.Y.; Zhang, Y.J. Study on damage size effect of cemented gangue backfill body under uniaxial compression. *Chin. J. Rock Mech. Eng.* **2021**, *40*, 2434–2444.
109. Feng, G.R.; Xie, W.S.; Guo, Y.X.; Guo, J.; Ran, H.Y.; Zhao, Y.H. Effect of early load on mechanical properties and damage of cemented gangue backfill. *Chin. J. Rock Mech. Eng.* **2021**, *41*, 775–784.
110. Zheng, B.C.; Zhou, H.Q.; He, R.J. Experimental Research on Coal Gangue Paste Filling Material. *Exp. Res. Coal Gangue Paste Fill. Mater.* **2006**, *4*, 460–463.
111. Wang, S.M.; Shen, Y.J.; Sun, Q.; Liu, L.; Shi, Q.M.; Zhu, M.B.; Zhang, B.; Cui, S.D. Underground CO₂ storage and technical problems in coal mining area under the “dual carbon” target. *J. China Coal Soc.* **2022**, *47*, 45–60.
112. Liu, L.; Wang, S.M.; Zhu, M.B.; Zhang, H.; Hou, D.Z.; Xun, C.; Zhang, X.Y.; Wang, X.L.; Wang, M. CO₂ storage-cavern construction and storage method based on functional backfill. *J. China Coal Soc.* **2022**, *47*, 1072–1086.
113. Yuan, L.; Jiang, Y.D.; He, X.Q.; Dou, L.M.; Zhao, X.P.; Zhao, X.S.; Wang, K.; Yu, Q.; Lu, X.M.; Li, H.C. Research progress of precise risk accurate identification and monitoring early warning on typical dynamic disasters in coal mine. *J. China Coal Soc.* **2018**, *43*, 306–318.
114. Xie, H.P.; Li, C.B.; Gao, M.Z.; Zhang, R.; Zhu, J.B. Conceptualization and preliminary research on deep in situ rock mechanics. *Chin. J. Rock Mech. Eng.* **2021**, *40*, 217–232.
115. Zhang, D.S.; Li, W.P.; Lai, X.P.; Fan, G. Development on basic theory of water protection during coal mining in northwest of China. *J. China Coal Soc.* **2017**, *42*, 36–43.
116. Woo, K.S.; Eberhardt, E.; Elmo, D.; Stead, D. Empirical investigation and characterization of surface subsidence related to block cave mining. *Int. J. Rock Mech. Min. Sci.* **2013**, *61*, 31–42. [[CrossRef](#)]

117. Ju, J.F.; Xu, J.L. Surface stepped subsidence related to top-coal caving longwall mining of extremely thick coal seam under shallow cover. *Int. J. Rock Mech. Min. Sci.* **2015**, *78*, 27–35. [[CrossRef](#)]
118. Tesarik, D.R.; Seymour, J.B.; Yanske, T.R. Long-term stability of a backfilled room-and-pillar test section at the Buick Mine, Missouri, USA. *Int. J. Rock Mech. Min. Sci.* **2009**, *46*, 1182–1196. [[CrossRef](#)]
119. Zeng, Q.; Li, G.S.; Dong, J.X.; Ya, P. Typical Ecological and Environmental Issues and Countermeasures in Coal Mining in Xinjiang Region. *Min. Saf. Environ. Prot.* **2017**, *44*, 106–110.
120. Li, Z.Y.; Cao, Y.W.; Ling, N.X.; Mei, Y.J. Compaction Mechanism of Aeolian Sand. *China J. Highw. Transp.* **2006**, *19*, 6–11.
121. Wang, X.D.; Xu, G.G.; Zhu, S.B.; Wu, B.Q.; Yuan, K.K. Rheological Properties of High Concentration Cemented Material Taking Loess and Aeolian Sand as Aggregates. *Safety* **2007**, *48*, 57–62.

Disclaimer/Publisher’s Note: The statements, opinions and data contained in all publications are solely those of the individual author(s) and contributor(s) and not of MDPI and/or the editor(s). MDPI and/or the editor(s) disclaim responsibility for any injury to people or property resulting from any ideas, methods, instructions or products referred to in the content.